

Differentially Private Fréchet Mean on the Manifold of Symmetric Positive Definite (SPD) Matrices

Saiteja Utpala*, Praneeth Vepakomma†, and Nina Miolane*

*UC Santa Barbara

†MIT

saitejautpala@gmail.com; vepakom@mit.edu ; ninamiolane@ucsb.edu

Abstract

Differential privacy has become crucial in the real-world deployment of statistical and machine learning algorithms with rigorous privacy guarantees. The earliest statistical queries, for which differential privacy mechanisms have been developed, were for the release of the sample mean. In Geometric Statistics, the sample Fréchet mean represents one of the most fundamental statistical summaries, as it generalizes the sample mean for data belonging to nonlinear manifolds. In that spirit, the only geometric statistical query for which a differential privacy mechanism has been developed, so far, is for the release of the sample Fréchet mean: the *Riemannian Laplace mechanism* was recently proposed to privatize the Fréchet mean on complete Riemannian manifolds. In many fields, the manifold of Symmetric Positive Definite (SPD) matrices is used to model data spaces, including in medical imaging where privacy requirements are key. We propose a novel, simple and fast mechanism - the *Tangent Gaussian mechanism* - to compute a differentially private Fréchet mean on the SPD manifold endowed with the log-Euclidean Riemannian metric. We show that our new mechanism obtains quadratic utility improvement in terms of data dimension over the current and only available baseline. Our mechanism is also simpler in practice as it does not require any expensive Markov Chain Monte Carlo (MCMC) sampling, and is computationally faster by multiple orders of magnitude — as confirmed by extensive experiments.

1 Introduction

Privacy-preserving computing is an active area of research which is necessitated by ethics, regulations, requirements for protections of trade secrets, or possible lack of trust amongst distributed data siloes. Privacy preservation is desired across several topologies of data sharing, be it from client devices to powerful centralized entities or a in peer-to-peer fashion. Mistrust in data sharing carries over not only in the sharing of raw data but also in the sharing of results obtained from intermediate or complete computations. The need for stringent privacy protections is often fueled by many privacy leakages and attacks that continue to happen under various settings operating without the right level of privacy-protecting mechanisms.

In this context, differential privacy (DP) Dwork et al. (2006); Dwork (2008); Dwork et al. (2014); Dwork (2006) has emerged as one of the leading mathematical definitions to ensure the preservation of privacy up to a chosen level. Privacy-preserving *mechanisms* that satisfy the definition of differential privacy were subsequently developed to privatize a wide range of statistical

and machine learning computations. The earliest queries, for which mechanisms have been proposed, were for the privatization of sample means in statistics, computed for data lying on linear spaces. When data belong to nonlinear manifolds, the Fréchet mean query Fréchet (1948) is the foundational building block of geometric statistics that needs to be privatized. Differentially private mechanisms for data lying on manifolds have not been extensively studied except for a work by Reimherr et al. (2021) that proposed a first mechanism for the private computation of Fréchet means. Our work proposes a new, simpler and faster, mechanism for private Fréchet means on the manifold of symmetric positive definite (SPD) matrices.

1.1 Motivation

Fréchet mean: a building block in geometric statistics While traditional statistics studies data that lies on *linear spaces*, geometric statistics studies data that lies on *nonlinear spaces* such as Riemannian manifolds, affine connection spaces, or stratified spaces Pennecc et al. (2019); Miolane (2016). Such analysis is fruitful as data might have inherent constraints that are well captured by the geometry of a nonlinear space. For instance, symmetric matrices constrained to have strictly positive eigenvalues are conveniently modeled as elements of the manifold of symmetric positive definite (SPD) matrices. Several extensions of traditional statistical analysis tools have thus been developed for the manifold setting: regression has been generalized to geodesic regression Fletcher (2011); Thomas Fletcher (2013), principal component analysis (PCA) to principal geodesic analysis or geodesic PCA Fletcher et al. (2004); Sommer et al. (2010); Huckemann et al. (2010), and mean shift to Riemannian mean shift clustering Subbarao and Meer (2009); Caseiro et al. (2012). In each of these algorithms, the computation of the *sample Fréchet mean* generalizes the computation of the *sample mean*, and thus represents the most fundamental building block. The privatization of the Fréchet mean is therefore the key element required to privatize geometric statistical queries. Privacy-preserving geometric statistics is also crucial, as one of its main application areas is medical imaging and computational anatomy Pennecc et al. (2019); Miolane (2016) for which privacy requirements are often desirable.

Importance of the SPD manifold with log-Euclidean metric Symmetric positive definite (SPD) matrices model a wide range of data, from medical images with Diffusion Tensor Imaging (DTI) Basser et al.; Pennecc et al. (2006), to physiological signals with electroencephalography (EEG) signals from brain-computer interfaces (BCI) Yger et al. (2016); Zanini et al. (2017); Chevallier et al. (2021), to 3D shapes Tabia et al. (2014) to name a few. Given their central roles for medical data where privacy is of the utmost importance Lotan et al. (2020); Li et al. (2005), private statistical computations on the SPD manifold are a worthy endeavour. The SPD manifold can be equipped with different *Riemannian metrics* that provide elementary operations such as distance computations. The log-Euclidean metric, originally proposed in Arsigny et al. (2006), has numerous advantages over another popular Riemannian metric called the affine invariant metric Pennecc et al. (2006): (a) it is computationally faster, (b) it gives similar or better performances on several processing and learning tasks, (c) and quite importantly, it provides a *closed form* expression for the Fréchet mean - which otherwise requires solving an optimization problem.

Need for better and faster privacy mechanisms Despite its importance for the processing of a number of (medical) data, geometric statistics currently stands understudied from the lens of differential privacy. The very recent work by Reimherr *et al* Reimherr et al. (2021) provides the first differentially private mechanism for the Fréchet mean. However, its utility - a measure of the mechanism's deviation from non-privatized computations - makes it impracticable on the manifold of SPD matrices as soon as we consider matrices of moderate size, e.g. 20×20 matrices.

Moreover, this mechanism is extremely expensive because it relies on MCMC sampling on the SPD manifold. Consequently, there is a need for better and faster privacy mechanisms on manifolds, starting with the SPD manifold.

1.2 Related Work and Contributions

To the best of our knowledge, the only existing work on differentially private geometric statistical queries is the mechanism by Reimherr *et al.* Reimherr et al. (2021) privatizing the Fréchet mean. The authors extend the standard Laplace mechanism Dwork et al. (2014) for linear spaces to complete Riemannian manifolds. Their *Riemannian Laplace mechanism* is based on a Laplace distribution that was originally proposed for SPD matrices Hajri et al. (2016) based on distance of the affine invariant metric Pennec et al. (2006), which they generalize to any manifold \mathcal{M} equipped with a distance ρ :

$$p(x) = \frac{1}{\mathcal{C}_{m,\sigma}} \exp\left(-\frac{\rho(x, m)}{\sigma}\right), \quad \forall x \in \mathcal{M} \quad (1)$$

where $m \in \mathcal{M}$, $\sigma \in \mathbb{R}_{>0}$ (positive reals) are parameters of the probability density p and $\mathcal{C}_{m,\sigma}$ is a normalizing constant. Reimherr *et al.* show that the mechanism obtained achieves pure differential privacy and provide an upper bound for the expectation of its utility (a measure of the deviation from non-privatized computations) for the Fréchet mean query. Their method is applicable to various Riemannian manifolds that satisfy some regularity conditions. We instead provide a privacy mechanism that is specific to the SPD manifold equipped with the log-Euclidean metric, but that gives a quadratic improvement in terms of utility, and is faster by several orders of magnitude. Table 1 summarizes the technical differences between Reimherr et al. (2021) and our work.

Mechanism \mathbf{A}	DP	Sampling	$\mathbb{E}[\rho^2(f(\mathcal{D}), \mathbf{A}(\mathcal{D}))]$	Theoretical Results
Riemannian Laplace Reimherr et al. (2021)	Pure DP	MCMC (expensive)	$\mathcal{O}(k^4)$	Expectation of $\rho^2(f(\mathcal{D}), \mathbf{A}(\mathcal{D}))$
Tangent Gaussian (Ours)	Approx. DP	Direct Sampling	$\mathcal{O}(\ln(1.25/\delta)k^2)$	Exact Distribution of $\rho^2(f(\mathcal{D}), \mathbf{A}(\mathcal{D}))$

Table 1: Differences between existing Reimherr et al. (2021) and proposed mechanisms for private Fréchet mean queries on the manifold of $k \times k$ SPD matrices endowed with the log-Euclidean metric. The notation $\rho^2(f(\mathcal{D}), \mathbf{A}(\mathcal{D}))$ represents the utility with \mathcal{D} the dataset, \mathbf{A} the mechanism under consideration, ρ the log-Euclidean distance, f the Fréchet mean and δ quantifies approximate differential privacy.

Our contributions are as follows.

1. We propose a new and simple mechanism - called the *Tangent Gaussian Mechanism* - that privatizes any statistical summary on the manifold of Symmetric Positive Definite (SPD) matrices endowed with the log-Euclidean metric. We prove that it achieves approximate differential privacy.
2. When the statistical summary is the Fréchet mean, we show that our mechanism obtains significant improvement in terms of utility over recent work - which we demonstrate theoretically, and practically for data in higher dimensions. Further, our mechanism is computationally simple, does not rely on additional parameters, and is multiple orders of magnitude faster than the state-of-the-art: *e.g.* nearly 4 orders of magnitude faster than Reimherr et al. (2021) on 30×30 SPD matrices.

3. We present the effectiveness of our mechanism on synthetic and real-world (medical) imaging data, the latter being represented via their covariance descriptors. To this aim, we also prove a theoretical bound on the radius of log-Euclidean geodesic ball with the covariance descriptor pipeline Tuzel et al. (2006) - required for the applicability of our mechanism.

2 Preliminaries and Notations

Elements of Riemannian Geometry Let \mathcal{M} be a d -dimensional smooth connected manifold and $T_p\mathcal{M}$ be its tangent space at point $p \in \mathcal{M}$. A *Riemannian metric* g on M is a collection of inner products $g_p : T_p\mathcal{M} \times T_p\mathcal{M} \rightarrow \mathbb{R}$ that vary smoothly with p . A manifold \mathcal{M} equipped with a Riemannian metric g is called a Riemannian manifold. Importantly, the metric g gives a distance ρ on \mathcal{M} . Let $\gamma : [0, 1] \rightarrow \mathcal{M}$ be a smooth parametrized curve on \mathcal{M} with velocity vector at t denoted as $\dot{\gamma}_t \in T_{\gamma(t)}\mathcal{M}$. The length of γ is defined as $L_\gamma = \int_0^1 \sqrt{g_{\gamma(t)}(\dot{\gamma}_t, \dot{\gamma}_t)} dt$ and the distance ρ between any two points $p, q \in \mathcal{M}$ is: $\rho(p, q) = \inf_{\gamma: \gamma(0)=p, \gamma(1)=q} L_\gamma$.

If in addition \mathcal{M} is complete for ρ , then any two points $p, q \in \mathcal{M}$ can be joined by length-minimizing curve, called a geodesic. We refer the reader to Do Carmo and Flaherty Francis (1992); Lee (2006); Helgason (1979) for a detailed exposition.

Elements of Differential Privacy (DP) Let \mathcal{X} be an input data space and \mathcal{M} the manifold under consideration. Let $f : \mathcal{X}^n \rightarrow \mathcal{M}$ be a manifold-valued statistical summary that requires privatization with respect to some sensitive dataset \mathcal{D} of size n , *i.e.* $\mathcal{D} \in \mathcal{X}^n$. Two datasets $\mathcal{D}, \mathcal{D}' \in \mathcal{X}^n$ are said to be adjacent if they differ by at most one data point. We denote adjacency as $\mathcal{D} \sim \mathcal{D}'$. The *sensitivity* of the summary f with respect to the distance ρ on \mathcal{M} is defined as:

$$\Delta_\rho = \sup_{\mathcal{D} \sim \mathcal{D}'} \rho(f(\mathcal{D}), f(\mathcal{D}')), \quad (2)$$

which is the maximum amount of deviation that can occur in the output of f for adjacent datasets.

A *mechanism* $\mathbf{A} : \mathcal{X}^n \rightarrow \mathcal{M}$ is a randomized algorithm that takes a dataset \mathcal{D} as input, and outputs a privatized version of the summary f on \mathcal{D} . The mechanism \mathbf{A} satisfies $(\epsilon, 0)$ differential privacy (also *pure differential privacy*) if, for all adjacent datasets $\mathcal{D} \sim \mathcal{D}'$ and for all measurable sets S of \mathcal{M} the following holds:

$$\mathbb{P}[\mathbf{A}(\mathcal{D}) \in S] \leq \exp(\epsilon) \mathbb{P}[\mathbf{A}(\mathcal{D}') \in S] \quad (3)$$

The intuition is that the change of a single element of the data space \mathcal{X} does not significantly alter the output distribution of the mechanism. As a relaxation, the mechanism \mathbf{A} satisfies (ϵ, δ) -differential privacy (also *approximate differential privacy*) if, for all adjacent datasets $\mathcal{D} \sim \mathcal{D}'$ and for all measurable sets S of \mathcal{M} :

$$\mathbb{P}[\mathbf{A}(\mathcal{D}) \in S] \leq \exp(\epsilon) \mathbb{P}[\mathbf{A}(\mathcal{D}') \in S] + \delta.$$

Intuitively, δ can be thought of as the probability of privacy failure, when Eq. (3) is not guaranteed.

Let $p_{\mathbf{A}(\mathcal{D})}$ be the density of the random variable $Y = \mathbf{A}(\mathcal{D})$. Given adjacent datasets $\mathcal{D} \sim \mathcal{D}'$, the *privacy loss function* of \mathbf{A} is defined as

$$\ell_{\mathbf{A}, \mathcal{D}, \mathcal{D}'}(y) = \ln \left(\frac{p_{\mathbf{A}(\mathcal{D})}(y)}{p_{\mathbf{A}(\mathcal{D}')} (y)} \right) \quad \forall y \in \mathcal{M}, \quad (4)$$

and the *privacy loss random variable* is $L_{\mathbf{A}, \mathcal{D}, \mathcal{D}'} = \ell_{\mathbf{A}, \mathcal{D}, \mathcal{D}'}(Y)$ Balle and Wang (2018). Importantly for our derivations, both sufficient and necessary conditions for the mechanism \mathbf{A} to be (ϵ, δ) -differentially private (DP) can be formulated in terms of $L_{\mathbf{A}, \mathcal{D}, \mathcal{D}'}$. The sufficient condition writes : $\forall \mathcal{D} \sim \mathcal{D}' : \mathbb{P}[L_{\mathbf{A}, \mathcal{D}, \mathcal{D}'} \geq \epsilon] \leq \delta \implies \mathbf{A}$ is (ϵ, δ) -DP. The sufficient & necessary condition is: $\forall \mathcal{D} \sim \mathcal{D}' : \mathbb{P}[L_{\mathbf{A}, \mathcal{D}, \mathcal{D}'} \geq \epsilon] - \exp(\epsilon) \mathbb{P}[L_{\mathbf{A}, \mathcal{D}, \mathcal{D}'} \leq -\epsilon] \leq \delta \iff \mathbf{A}$ is (ϵ, δ) -DP.

Fréchet Mean When the data space \mathcal{X} is equal to the manifold \mathcal{M} , we will be interested in mechanisms that can privatize a specific statistical summary f called the Fréchet mean. The sample Fréchet mean \bar{X} Fréchet (1948) of the dataset $\mathcal{D} = \{X_1, \dots, X_n\}$ on the manifold \mathcal{M} is defined as

$$\bar{X} \triangleq \left\{ p \mid p \in \arg \min_{q \in \mathcal{M}} \sum_{i=1}^n \rho^2(q, X_i) \right\},$$

i.e. we have in this case $\bar{X} = f(\mathcal{D})$ for $\mathcal{D} \in \mathcal{M}^n$. Intuitively, the Fréchet mean uses a property of the mean on linear spaces - namely the fact that mean minimizes the sum of squared distances to the data points - as a definition of mean on manifolds. Crucially, the Fréchet mean depends on the distance ρ and therefore on the Riemannian metric defined on \mathcal{M} . We also note that the Fréchet mean might not always exist, and if it exists it might not be unique – see supplementary materials. In practice, computing \bar{X} generally requires optimization algorithms such as gradient descent on manifolds Boumal (2020).

3 Geometry of the SPD Manifold with Log Euclidean Metric

Manifold and vector space structures We now restrict \mathcal{M} to be the manifold of symmetric positive definite (SPD) matrices:

$$\text{SPD}(k) = \left\{ X \in \mathbb{R}^{k \times k} \mid X^T = X \text{ and } \forall u \in \mathbb{R}^k \setminus \{0\}, u^T X u > 0 \right\}, \quad (5)$$

which has dimension $d = \frac{k(k+1)}{2}$. The tangent space of the manifold $\text{SPD}(k)$ at any point $X \in \text{SPD}(k)$ is the vector space of symmetric matrices $\text{SYM}(k)$. The mathematical construct $(\text{SPD}(k), +, \cdot)$ is not a vector space under element-wise addition and element-wise scalar multiplication. This can be seen from the observation that $a \in \mathbb{R}_{\leq 0}, X \in \text{SPD}(k) \implies aX \notin \text{SPD}(k)$. Instead, $\text{SPD}(k)$ is an open cone of $\mathbb{R}^{k \times k}$ and, as such, naturally possesses a smooth manifold structure which can further be equipped with different Riemannian metrics Thanwerdas and Penec (2021). However, Arsigny *et al.* Arsigny *et al.* (2007) showed in a surprising result that $\text{SPD}(k)$ can be given a vector space structure $(\text{SPD}(k), \oplus, \odot)$ via the operations \oplus, \odot defined in Table 2, where $\text{Exp}_m, \text{Log}_m$ denote the matrix exponential and matrix logarithm. This fact is central for the proofs provided in the present paper.

Riemannian structure Arsigny *et al.* further define a Riemannian metric on $\text{SPD}(k)$, called the *log-Euclidean metric*, which induces the following distance:

$$\rho_{\text{LE}}(X_1, X_2) = \|\text{Log}_m X_1 - \text{Log}_m X_2\|_F, \quad \forall X_1, X_2 \in \text{SPD}(k), \quad (6)$$

where $\|\cdot\|_F$ denotes the Frobenius norm on matrices. Importantly, the log-Euclidean metric Arsigny *et al.* (2006) gives a unique and simple closed form expression for the Fréchet mean in terms of matrix logarithm and matrix exponential

$$\bar{X}_{\text{LE}} = \text{Exp}_m \left[\frac{1}{n} \sum_{i=1}^n \text{Log}_m X_i \right],$$

OPERATION	NOTATION	EXPRESSION
Addition	$X_1 \oplus X_2$	$\text{Expm} [\text{Logm } X_1 + \text{Logm } X_2]$
Subtraction	$X_1 \ominus X_2$	$\text{Expm} [\text{Logm } X_1 - \text{Logm } X_2]$
Scalar Multiplication	$a \odot X$	$\text{Expm} [a \cdot \text{Logm } X]$

Table 2: Operations turning the manifold $\text{SPD}(k)$ into a vector space. Expm and Logm denote the matrix exponential and logarithms, respectively. X_1, X_2 belong to $\text{SPD}(k)$ while $a \in \mathbb{R}$ is a scalar.

for the dataset $X_1, \dots, X_n \in \text{SPD}(k)$.

Maps between spaces Lastly, we present maps that will help us define the differential privacy mechanism proposed in the next section. Consider the map $\text{vecd} : \text{SYM}(k) \rightarrow \mathbb{R}^{\frac{k(k+1)}{2}}$ defined as $\text{vecd}(X) = [\text{diag}(X)^T, \sqrt{2} \text{upperdiag}(X)^T]^T$, where $\text{diag} : \text{SYM}(k) \rightarrow \mathbb{R}^k$ and $\text{upperdiag} : \text{SYM}(k) \rightarrow \mathbb{R}^{\frac{k(k-1)}{2}}$ build vectors from the diagonal, and from the strictly upper diagonal entries, of the matrix X . The map vecd is invertible and we denote by invvecd its inverse. Specifically, the spaces $\text{SPD}(k), \text{SYM}(k)$ and $\mathbb{R}^{\frac{k(k+1)}{2}}$ are now related as follows:

$$\text{SPD}(k) \begin{array}{c} \xleftarrow{\text{Logm}} \\ \xrightarrow{\text{Expm}} \end{array} \text{SYM}(k) \begin{array}{c} \xleftarrow{\text{vecd}} \\ \xrightarrow{\text{invvecd}} \end{array} \mathbb{R}^{\frac{k(k+1)}{2}}.$$

4 Tangent Gaussian Mechanism on SPD manifolds

We can now introduce our differential privacy mechanism for statistical summaries on the $\text{SPD}(k)$ manifold. Let $f : \mathcal{X}^n \rightarrow \text{SPD}(k)$ be any $\text{SPD}(k)$ -valued summary that needs to be privatized. The proposed mechanism is based on the log Gaussian distribution on the SPD manifold Schwartzman (2016) which is defined as follows. Consider a mean $M \in \text{SPD}(k)$ and a tangent covariance $\Sigma \in \text{SPD}\left(\frac{k(k+1)}{2}\right)$. We can (i) first map the mean M to the tangent space $\text{SYM}(k)$ of $\text{SPD}(k)$ at the identity using the matrix Logarithm Logm , then (ii) to $\mathbb{R}^{\frac{k(k+1)}{2}}$ using the map vecd introduced in the previous section, and (iii) consider whether the result follows a traditional Gaussian distribution.

Definition 1 (Log Gaussian Distribution on $\text{SPD}(k)$ Schwartzman (2016)). *Given a mean $M \in \text{SPD}(k)$, and a tangent covariance $\Sigma \in \text{SPD}\left(\frac{k(k+1)}{2}\right)$, we say that $X \sim \mathcal{LN}(M, \Sigma)$ follows a log Gaussian distribution on $\text{SPD}(k)$ if $\text{vecd}[\text{Logm } X] \sim \mathcal{N}(\text{vecd}[\text{Logm } M], \Sigma)$ follows a (regular) Gaussian distribution with mean $\text{vecd} \text{Logm } M$ and covariance matrix Σ on $\mathbb{R}^{\frac{k(k+1)}{2}}$.*

The density $p(X|M, \Sigma)$ is then given by

$$\frac{J(X)}{(2\pi)^{\frac{d}{2}} (\det \Sigma)^{\frac{1}{2}}} \exp\left(-\frac{1}{2} \text{vecd}(\text{Logm } X - \text{Logm } M)^T \Sigma^{-1} \text{vecd}(\text{Logm } X - \text{Logm } M)\right)$$

where $d = \frac{k(k+1)}{2}$, $J(X) = \frac{1}{\det X} \prod_{i < j} h(\lambda_i, \lambda_j)$, and $h(\lambda_i, \lambda_j) = \begin{cases} (\log \lambda_i - \log \lambda_j) & \lambda_i > \lambda_j \\ \frac{1}{\lambda_i} & \lambda_i = \lambda_j \end{cases}$, with λ_i, λ_j eigenvalues of the matrix X .

Algorithm 1: Tangent Gaussian Mechanism for $f : \mathcal{X}^n \rightarrow \text{SPD}(k)$

- 1 **function** Tangent Gaussian Mechanism (\mathcal{D} , sigma-type, Δ_{LE} , ϵ , δ);
 Inputs : Dataset \mathcal{D} of $k \times k$ SPD matrices of size n , sigma-type $\in \{\text{'classical'}, \text{'analytic'}\}$
 Δ_{LE} the log-Euclidean sensitivity of f , $\epsilon > 0$, $\delta \in (0, 1)$ and additionally $\epsilon < 1$ if
 sigma-type is 'classical'.
 Output: Private $f(\mathcal{D})$
 - 2 **if** sigma-type is 'classical' **then** $\sigma = \text{CLASSIC}(\Delta_{\text{LE}}, \epsilon, \delta)$; **else** $\sigma = \text{ANALYTIC}(\Delta_{\text{LE}}, \epsilon, \delta)$;
 - 3 Compute non private output : $f_{\text{np}} := f(\mathcal{D})$
 - 4 Compute mean of Gaussian distribution: $M := \text{vecd}[\text{Logm } f_{\text{np}}]$, $M \in \mathbb{R}^{\frac{k(k+1)}{2}}$
 - 5 Sample from the Gaussian distribution in $\mathbb{R}^{\frac{k(k+1)}{2}}$: $N \sim \mathcal{N}(M, \sigma^2 I)$
 - 6 Map sample to the SPD manifold: $f_p := \text{Expm}[\text{invvecd } N]$
 - 7 Return private f_p
-

The definition of log Gaussian distribution on the $\text{SPD}(k)$ manifold allows us to define our proposed Tangent Gaussian mechanism.

Definition 2 (Tangent Gaussian Mechanism). *Consider any statistical summary $f : \mathcal{X}^n \rightarrow \text{SPD}(k)$ on the manifold $\text{SPD}(k)$ equipped with log-Euclidean metric. Given $\sigma^2 > 0$, we define the Tangent Gaussian mechanism $\mathbf{A}_{\text{TG}} : \mathcal{X}^n \rightarrow \text{SPD}(k)$, as*

$$\mathbf{A}_{\text{TG}}(\mathcal{D}) = X, \text{ where } X \sim \mathcal{LN}(f(\mathcal{D}), \sigma^2 I).$$

We now state our main theorem, which shows that the privacy loss of the Tangent Gaussian mechanism is normally distributed with mean and variance parametrized by the log-Euclidean distance.

Theorem 3 (Distribution of Privacy Loss for the Tangent Gaussian Mechanism). *Let \mathbf{A}_{TG} be a Tangent Gaussian mechanism with variance σ^2 . Its privacy loss is normally distributed as*

$$L_{\mathbf{A}_{\text{TG}}, \mathcal{D}, \mathcal{D}'} \sim \mathcal{N}\left(\frac{\rho_{\text{LE}}^2(f(\mathcal{D}), f(\mathcal{D}'))}{2\sigma^2}, \frac{\rho_{\text{LE}}^2(f(\mathcal{D}), f(\mathcal{D}'))}{\sigma^2}\right).$$

This distribution is analogous to the distribution of the privacy loss for the Euclidean Gaussian mechanism, but with the log-Euclidean sensitivity instead of the Euclidean sensitivity Dwork et al. (2014); Balle and Wang (2018). Consequently, our theoretical analysis of the Tangent Gaussian mechanism - deriving privacy guarantees from the distribution of the privacy loss above - closely follows the steps of the analysis for the Euclidean Gaussian case. Specifically, we can proceed in two ways with either a (1) classical approach where sufficient conditions are used to show the mechanism is (ϵ, δ) -DP as in Dwork et al. (2014), or with an (2) analytic approach where the utility is better by using sufficient and necessary conditions Balle and Wang (2018).

Theorem 4 (Privacy Guarantee of Tangent Gaussian Mechanism). *Consider $f : \mathcal{X}^n \rightarrow \text{SPD}(k)$ with log-Euclidean sensitivity Δ_{LE} .*

1. (Classical) Given $\epsilon, \delta \in (0, 1)$, choosing $\sigma = \Delta_{\text{LE}} \sqrt{2 \ln(1.25/\delta)}/\epsilon$, makes the Tangent Gaussian mechanism (ϵ, δ) -differentially private.

2. (Analytic) Given $\epsilon \geq 0, \delta \in (0, 1)$ and Φ the cumulative distribution of the standard Gaussian, choosing any σ that satisfies $\Phi(\frac{\Delta_{\text{LE}}}{2\sigma} - \frac{\epsilon\sigma}{\Delta_{\text{LE}}}) - \exp(\epsilon)\Phi(\frac{\Delta_{\text{LE}}}{2\sigma} - \frac{\epsilon\sigma}{\Delta_{\text{LE}}}) \leq \delta$ makes the Tangent Gaussian mechanism (ϵ, δ) -differentially private.

Proofs are in the supplementary materials. Algorithm 1 shows the implementation of the mechanism.

5 Privatizing the Fréchet mean

In the previous section, f is any function that outputs a summary statistics on $\text{SPD}(k)$. In this section, we seek to privatize the Fréchet mean f of the log-Euclidean metric. We first compute its sensitivity and then provide its utility. In what follows, $\mathcal{B}_r(M) = \{X | \rho_{\text{LE}}(M, X) < r\}$ denotes an open geodesic ball of radius $0 < r < \infty$ centered at $M \in \text{SPD}(k)$.

Theorem 5 (Sensitivity of Log-Euclidean Fréchet Mean). *Given data in $\mathcal{B}_r(M)$ for some $0 < r < \infty$ and $M \in \text{SPD}(k)$, the sensitivity of the log-Euclidean Fréchet mean verifies: $\Delta_{\text{LE}} \leq \frac{2r}{n}$.*

The utility of the Tangent Gaussian mechanism for a Fréchet mean query is then given below.

Theorem 6 (Utility). *Let \mathbf{A}_{TG} be the (classical) Tangent Gaussian mechanism, $\mathcal{B}_r(M)$ a geodesic ball of radius $0 < r < \infty$ and center $M \in \mathcal{M}$ containing the dataset \mathcal{D} and f the Fréchet mean. The utility of the mechanism \mathbf{A}_{TG} is given by:*

$$\begin{aligned} \rho_{\text{LE}}^2(f(\mathcal{D}), \mathbf{A}_{\text{TG}}(\mathcal{D})) &\sim \sigma^2 \chi_d^2, \\ \mathbb{E}[\rho_{\text{LE}}^2(f(\mathcal{D}), \mathbf{A}_{\text{TG}}(\mathcal{D}))] &= \frac{4r^2 \ln(1.25/\delta)d}{n^2 \epsilon^2} \quad \text{with } d = \dim(\text{SPD}(k)) = \frac{k(k+1)}{2}, \end{aligned}$$

where χ_d^2 represents the chi squared distribution with d degree of freedoms.

Proofs are in the supplementary materials. We compare these results with those of the Riemannian Laplace mechanism Reimherr et al. (2021), denoted \mathbf{A}_{RL} .

Utility: The utility of the Riemannian Laplace mechanism has an expectation given by $\mathbb{E}[\rho_{\text{LE}}^2(f(\mathcal{D}), \mathbf{A}_{\text{RL}}(\mathcal{D}))] = \mathcal{O}(\frac{r^2 d^2}{n^2 \epsilon^2}) = \mathcal{O}(k^4)$. By contrast, our Tangent Gaussian mechanism provides $\mathbb{E}[\rho_{\text{LE}}^2(f(\mathcal{D}), \mathbf{A}_{\text{TG}}(\mathcal{D}))] = \mathcal{O}(\ln(1.25/\delta)k^2)$, which represents a quadratic improvement. Our comparison here uses ρ^2 instead of ρ because Reimherr et al. (2021) derives the utility for Riemannian Laplace mechanism with ρ^2 instead of ρ . The interested reader can apply Jensen's inequality $\mathbb{E}[\rho] \leq \sqrt{\mathbb{E}[\rho^2]}$ to get a naive bound on $\mathbb{E}[\rho]$. As this could be a loose bound, we prefer to use ρ_{LE}^2 to compare utilities in our theoretical results. However, our experiments will compare sample utility with ρ_{LE} . Note that, regardless of whether one compares ρ or ρ^2 , our method still obtains a quadratic improvement.

Effect of δ : The Riemannian Laplace mechanism is pure DP, whereas our mechanism is approximate DP. This means that our utility depends on δ as well. However, the dependency has the form $\ln(1.25/\delta)$ which is an extremely slow changing function of δ . For instance, changing δ from 10^{-9} to 10^{-18} increases $\ln(1.25/\delta)$ from 2.4 to 3.1. Thus, approximate DP is not an obstacle in practice.

Theoretical Results: The authors of Reimherr et al. (2021) characterize the utility of the Riemannian Laplace mechanism in terms of its expectation $\mathbb{E}[\rho_{\text{LE}}^2(f(\mathcal{D}), \mathbf{A}(\mathcal{D}))]$. By contrast, our results yield a more complete picture, as we derive the probability distribution of $\rho_{\text{LE}}^2(f(\mathcal{D}), \mathbf{A}(\mathcal{D}))$.

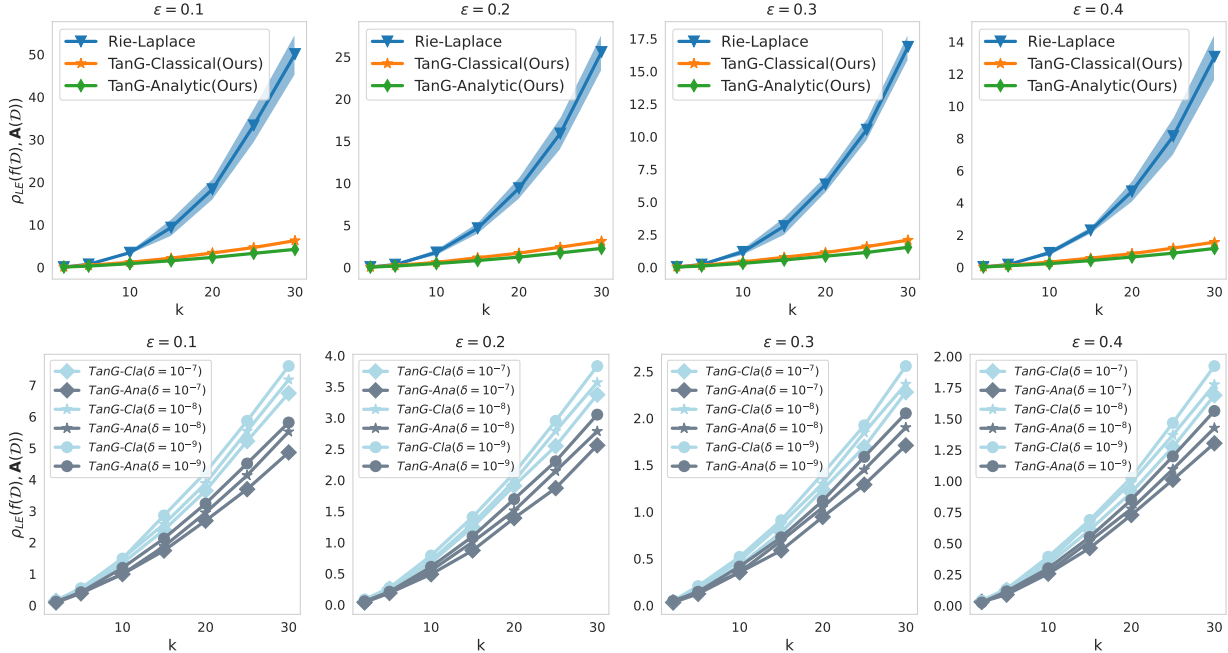


Figure 1: Utilities on synthetic data for *Rie-Laplace* the Riemannian Laplace mechanism Reimherr et al. (2021), and *TanG Classical*, *TanG-Cla* and *TanG Analytic*, *TanG-Ana* our proposed Tangent Gaussian mechanisms (classical and analytic versions) for different matrix sizes k and privacy parameter ϵ .

6 Experiments

We privatize the Fréchet mean with our two newly proposed mechanisms from Th. 13 (1) Tangent Gaussian Classical and (2) Tangent Gaussian Analytic, as well as with the Riemannian Laplace mechanism Reimherr et al. (2021) used as baseline. Privatizing the log-Euclidean Fréchet mean with the Riemannian Laplace mechanism requires sampling from Riemannian Laplace distribution (parametrized with log-Euclidean distance Eq. (25)), which necessitates a costly MCMC procedure. Our experiments rely on the software *Geomstats* for the computation of differential geometry’s operations Miolane et al. (2020a,b) and the code is provided in the supplementary materials.

6.1 Experiments on Synthetic Datasets

The utility depends on privacy parameters (ϵ, δ) , the size k of the matrices, the dataset size n and r the radius of the geodesic ball containing the dataset. The utilities of the Tangent Gaussian and Riemannian Laplace mechanisms have the same dependency on n, ϵ, r , such that their differentiating parameters are δ, k . Consequently, our experiments on synthetic data fix n, ϵ, r and vary δ, k .

We generate random $k \times k$ SPD matrices as follows: (i) generate k real values $(\lambda_1, \dots, \lambda_k)$ uniformly in $[e^{-r}, e^r]$, (ii) build D the diagonal matrix with $D_{ii} = \lambda_i$, for $i \in \{1, \dots, k\}$, (iii) generate a $k \times k$ random orthogonal matrix E with the Haar distribution, and (iv) build the SPD matrix as: $X = EDE^T$. This process generates SPD matrices, that can be shown to belong to the geodesic ball $\mathcal{B}_{\sqrt{kr}}(I)$ with I the identity matrix: $\|\text{Logm } X\|_F = \sqrt{\sum_{i=1}^k (\ln \lambda_i)^2} \leq \sqrt{kr^2} = \sqrt{kr}$.

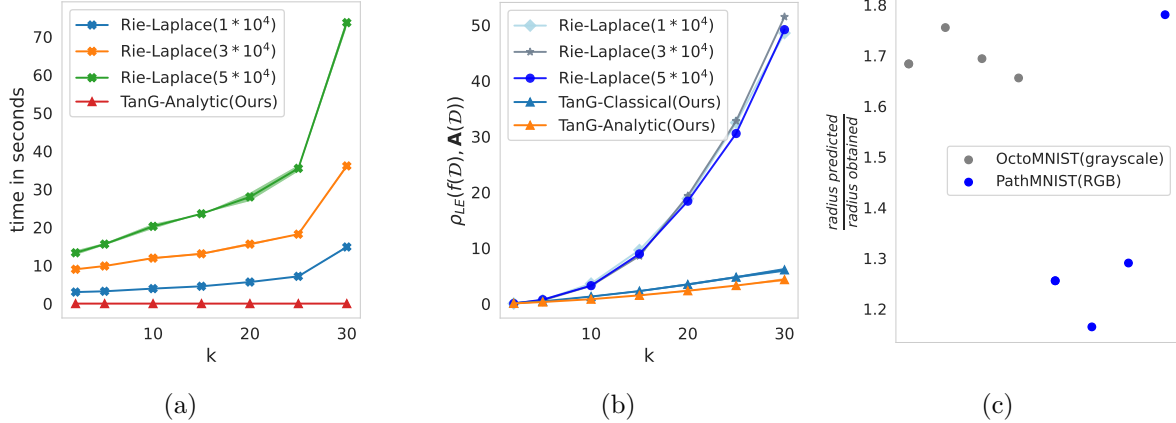


Figure 2: (a) Computational times for *Rie-Laplace*(x) the Riemannian Laplace mechanism with a MCMC burn-in of $x \in \{10,000; 30,000; 50,000\}$ Reimherr et al. (2021), and *TanG-Analytic* the proposed Tangent Gaussian mechanism (analytic version). (b) Utility with varying burn-ins for *Rie-Laplace*. Plots (a, b) use different matrix sizes k . Plot (c) explores if the bound from Th. 7 is tight in practice.

We use $n = 500$ and $r = 1/4$ such that Th. 5 yields the following sensitivity for the Fréchet mean: $\Delta \leq (2 * \sqrt{k}) / (4 * 500) = \sqrt{k} / 1000$.

Fig. 1 (top) compares utilities using a fixed $\delta = 10^{-6}$ for our mechanism, a MCMC burn-in of 50,000 for the Riemannian Laplace mechanism, and different values of $k \in \{2, 5, 10, 15, 20, 25, 30\}$ and $\epsilon \in \{0.1, 0.2, 0.3, 0.4\}$. Each experiment is repeated 10 times, the results are averaged and the (avg-2*std, avg+2*std) band is shown. The std is small for our mechanism, and does not appear on the plots. The Tangent Gaussian mechanisms (ours) yield almost $\times 10$ utility improvement for larger k , for each ϵ . Fig. 1 (bottom) shows that, as expected, our utility is not significantly impacted by different values of $\delta \in \{10^{-7}, 10^{-8}, 10^{-9}\}$.

We compare the times required to privatize the Fréchet mean using both mechanisms and varying $k \in \{2, 5, 10, 15, 20, 25, 30\}$ in Fig. 2(a). Since the Riemannian Laplace relies on MCMC, its time depends on the burn-in - that we choose in $\{10000, 30000, 50000\}$. For $k = 30$, Fig. 2(a) shows that Riemannian Laplace mechanism takes 14 sec (burn-in 10000), 36 sec (burn-in 30000) and 73 sec (burn-in 50000) - whereas our Tangent Gaussian (Analytic) mechanism takes 1.3 *microsec*, i.e. is nearly $\times 9979$ (burn-in 10000), $\times 24265$ (burn-in 30000), and $\times 49521$ (burn-in 50000) faster than the Riemannian Laplace. Fig. 2(b) considers the effect of the burn-in on the Riemannian Laplace’s utility and finds no significant difference for burn-ins in $\{10000, 30000, 50000\}$.

6.2 Experiments on Real-World Datasets

We run experiments on covariance descriptors of real-world (medical) images. Covariance descriptors Tuzel et al. (2006) have been widely used for face and person recognition Tuzel et al. (2007); Zhang and Li (2011); Pang et al. (2008); Križaj et al. (2013); Ma et al. (2014); Cai et al. (2010); Zeng et al. (2015); Matsukawa et al. (2016), action and gesture recognition Cirujeda and Binefa (2014); Hussein et al. (2013); Sharaf et al. (2015), 3D shape analysis Tabia et al. (2014); Ma et al. (2014), medical imaging Khan et al. (2015); Cirujeda et al. (2016); and even recently as layers in neural networks Yu and Salzmann (2017) - which makes them interesting data to privatize.

Let $\mathcal{I} \in \mathbb{R}^{h \times w \times c}$ be an image of height h , width w and with c channels, where c is 1 for gray

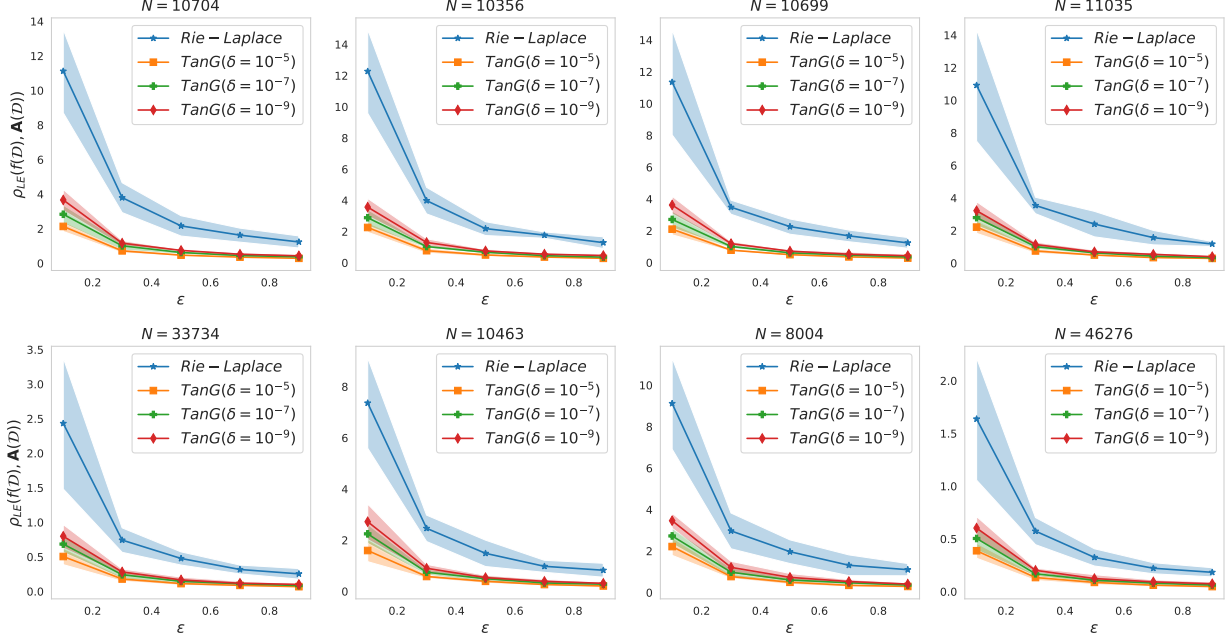


Figure 3: Utilities on the private Fréchet means for different privacy parameters ϵ , and real-world datasets of sizes N . Top: PathMNIST (RGB images yielding 11×11 SPD descriptors). Bottom: OctoMNIST (gray scale images yielding 9×9 SPD matrices). *Rie-Laplace* is the Riemannian Laplacian mechanism Reimherr et al. (2021) and *TanG* the Tangent Gaussian mechanism for different values of δ (ours). We also show the mean-2*std, mean+2*std bands.

scale images and 3 for RGB images. Let $\phi : \mathbb{R}^{h \times w \times c} \rightarrow \mathbb{R}^{hw \times k}$ be a feature extractor of dimension k , i.e. $\phi(\mathcal{I})(\mathbf{x})$ is a k -dimensional vector at each spatial coordinate \mathbf{x} in the image's domain S . Given a small $\eta > 0$, the *covariance descriptor* $\mathbf{R}_\eta : \mathbb{R}^{h \times w \times c} \rightarrow \text{SPD}(k)$ associated with ϕ is defined as

$$\mathbf{R}_\eta(\mathcal{I}) = \left[\frac{1}{|S|} \sum_{\mathbf{x} \in S} (\phi(\mathcal{I})(\mathbf{x}) - \mu)(\phi(\mathcal{I})(\mathbf{x}) - \mu)^T \right] + \eta \cdot I,$$

where $\mu = |S|^{-1} \sum_{\mathbf{x} \in S} \phi(\mathcal{I})(\mathbf{x})$, and $\eta \cdot I$ ensures $\mathbf{R}_\eta(\mathcal{I}) \in \text{SPD}(k)$ with η usually set to 10^{-6} . Our experiments follow Tuzel et al. (2006); Jayasumana et al. (2015) and use the covariance descriptors with the feature vector as $\phi(\mathcal{I})(\mathbf{x}) = \left[x, y, \mathcal{I}, |\mathcal{I}_x|, |\mathcal{I}_y|, |\mathcal{I}_{xx}|, |\mathcal{I}_{yy}|, \sqrt{|\mathcal{I}_x|^2 + |\mathcal{I}_y|^2}, \arctan\left(\frac{|\mathcal{I}_x|}{|\mathcal{I}_y|}\right) \right]$, where $\mathbf{x} = (x, y)$, intensities derivatives are denoted by $\mathcal{I}_x, \mathcal{I}_y, \mathcal{I}_{xx}, \mathcal{I}_{yy}$ and we added the intensity values \mathcal{I} for each channel compared to Tuzel et al. (2006); Jayasumana et al. (2015). For gray scale images, $\phi(\mathcal{I})(\mathbf{x})$ is a 9-dimensional vector that makes $\mathbf{R}_\eta(\mathcal{I})$ a 9×9 SPD matrix, while for RGB images $\phi(\mathcal{I})(\mathbf{x})$ is a 11-dimensional vector that makes $\mathbf{R}_\eta(\mathcal{I})$ a 11×11 SPD matrix. We are within the assumptions of Th. 6 since such covariance descriptors belong to geodesic balls centered at I , as shown by the following theorem.

Theorem 7. Let $\mathbf{R}_\eta(\mathcal{I})$ be the covariance descriptor associated with the feature vector $\phi(\mathcal{I})$ above.

1. If \mathcal{I} is a gray scale image, then $\|\text{Logm } \mathbf{R}_\eta(\mathcal{I})\|_F \leq \sqrt{9} \max\{|\ln \eta|, |\ln(14 + \eta)|\}$.
2. If \mathcal{I} is a RGB image, then $\|\text{Logm } \mathbf{R}_\eta(\mathcal{I})\|_F \leq \sqrt{11} \max\{|\ln \eta|, |\ln(16 + \eta)|\}$.

We use images from 4 classes of the medical imaging datasets PATHMNIST (gray scale) and OctoMNIST (RGB) from MedMNISTv2 Yang et al. (2021), compute the 4 class-wise Fréchet means of their covariance descriptors ($\eta = 10^{-6}$), which we privatize using the Riemannian Laplace and Tangent Gaussian (analytical) mechanisms. Fig. 3 shows the utilities for different values of $\epsilon \in \{0.1, 0.3, 0.5, 0.7, 0.9\}$ and $\delta \in \{10^{-5}, 10^{-7}, 10^{-9}\}$. The datasets sizes N range from 8000 to 46276 images. The sensitivity of the Fréchet mean, required for the mechanisms, is calculated using Th. 7 and Th. 5. Each experiment is repeated 10 times and averaged, while the (avg-2*std, avg+ 2*std) band is shown. Our mechanism also outperforms the Riemannian Laplace on real-world datasets, and the utility gap is higher for smaller values of N and ϵ . Fig. 2 (c) shows that the bound derived in Th. 7 is tight in practice, as illustrated by the ratio of the bound obtained in Th.7 and the practical bound. Experiments on additional real-world datasets are in the supplementary materials.

7 Conclusion and Future Work

Differential privacy for geometric statistics and learning is at a very early stage. We proposed a Tangent Gaussian mechanism that is specific to the SPD manifold equipped with the log-Euclidean metric, and that outperforms the only existing baseline. One limitation of our work is that the proposed mechanism is restricted to one manifold with one specific metric. While the log-Euclidean metric is one of the most important metrics on the SPD manifold, future work should investigate how to build a Gaussian mechanism that works on any complete Riemannian manifold. We could define such as a mechanism using a Riemannian Gaussian distribution derived in Pennec (2006). The main challenge would be to show that the associated procedure is (ϵ, δ) differentially private. Future work can also seek to privatize other geometric statistical algorithms like geodesic regression or principal geodesic analysis.

References

- Bijan Afsari. Riemannian \mathcal{L}^p center of mass: existence, uniqueness, and convexity. *Proceedings of the American Mathematical Society*, 139(2):655–673, 2011. 28
- Vincent Arsigny, Pierre Fillard, Xavier Pennec, and Nicholas Ayache. Log-euclidean metrics for fast and simple calculus on diffusion tensors. *Magnetic Resonance in Medicine: An Official Journal of the International Society for Magnetic Resonance in Medicine*, 56(2):411–421, 2006. 2, 5
- Vincent Arsigny, Pierre Fillard, Xavier Pennec, and Nicholas Ayache. Geometric means in a novel vector space structure on symmetric positive-definite matrices. *SIAM journal on matrix analysis and applications*, 29(1):328–347, 2007. 5
- Borja Balle and Yu-Xiang Wang. Improving the gaussian mechanism for differential privacy: Analytical calibration and optimal denoising. In *International Conference on Machine Learning*, pages 394–403. PMLR, 2018. 5, 7, 20
- P. J. Basser, J. Mattiello, and D. Le Bihan. MR diffusion tensor spectroscopy and imaging. *Biophysical Journal*, 66(1):259–67. URL <https://hal.archives-ouvertes.fr/hal-00349721>. 2
- Nicolas Boumal. An introduction to optimization on smooth manifolds. *Available online*, May, 3, 2020. 5

- Yinghao Cai, Valtteri Takala, and Matti Pietikainen. Matching groups of people by covariance descriptor. In *2010 20th International Conference on Pattern Recognition*, pages 2744–2747. IEEE, 2010. 10
- Rui Caseiro, Joao F Henriques, Pedro Martins, and Jorge Batista. Semi-intrinsic mean shift on riemannian manifolds. In *European conference on computer vision*, pages 342–355. Springer, 2012. 2
- Sylvain Chevallier, Emmanuel K Kalunga, Quentin Barthélemy, and Eric Monacelli. Review of riemannian distances and divergences, applied to ssvp-based bci. *Neuroinformatics*, 19(1): 93–106, 2021. 2
- Pol Cirujeda and Xavier Binefa. 4dcov: A nested covariance descriptor of spatio-temporal features for gesture recognition in depth sequences. In *2014 2nd International Conference on 3D Vision*, volume 1, pages 657–664. IEEE, 2014. 10
- Pol Cirujeda, Yashin Dicente Cid, Henning Müller, Daniel Rubin, Todd A Aguilera, Billy W Loo, Maximilian Diehn, Xavier Binefa, and Adrien Depeursinge. A 3-d riesz-covariance texture model for prediction of nodule recurrence in lung ct. *IEEE transactions on medical imaging*, 35(12):2620–2630, 2016. 10
- Tarin Clanuwat, Mikel Bober-Irizar, Asanobu Kitamoto, Alex Lamb, Kazuaki Yamamoto, and David Ha. Deep learning for classical japanese literature. *arXiv preprint arXiv:1812.01718*, 2018. 26
- Manfredo Perdigao Do Carmo and J Flaherty Francis. *Riemannian geometry*, volume 6. Springer, 1992. 4
- Cynthia Dwork. Differential privacy. In Michele Bugliesi, Bart Preneel, Vladimiro Sassone, and Ingo Wegener, editors, *Automata, Languages and Programming*, pages 1–12, Berlin, Heidelberg, 2006. Springer Berlin Heidelberg. ISBN 978-3-540-35908-1. 1
- Cynthia Dwork. Differential privacy: A survey of results. In *International conference on theory and applications of models of computation*, pages 1–19. Springer, 2008. 1
- Cynthia Dwork, Frank McSherry, Kobbi Nissim, and Adam Smith. Calibrating noise to sensitivity in private data analysis. In *Theory of cryptography conference*, pages 265–284. Springer, 2006. 1
- Cynthia Dwork, Aaron Roth, et al. The algorithmic foundations of differential privacy. *Found. Trends Theor. Comput. Sci.*, 9(3-4):211–407, 2014. 1, 3, 7, 20
- P Thomas Fletcher, Conglin Lu, Stephen M Pizer, and Sarang Joshi. Principal geodesic analysis for the study of nonlinear statistics of shape. *IEEE transactions on medical imaging*, 23(8): 995–1005, 2004. 2
- Thomas Fletcher. Geodesic regression on riemannian manifolds. In *Proceedings of the Third International Workshop on Mathematical Foundations of Computational Anatomy-Geometrical and Statistical Methods for Modelling Biological Shape Variability*, pages 75–86, 2011. 2
- Maurice Fréchet. Les éléments aléatoires de nature quelconque dans un espace distancié. In *Annales de l'institut Henri Poincaré*, volume 10, pages 215–310, 1948. 2, 5

- Hatem Hajri, Ioana Ilea, Salem Said, Lionel Bombrun, and Yannick Berthoumieu. Riemannian laplace distribution on the space of symmetric positive definite matrices. *Entropy*, 18(3):98, 2016. 3
- Sigurdur Helgason. *Differential geometry, Lie groups, and symmetric spaces*. Academic press, 1979. 4
- Stephan Huckemann, Thomas Hotz, and Axel Munk. Intrinsic shape analysis: Geodesic pca for riemannian manifolds modulo isometric lie group actions. *Statistica Sinica*, pages 1–58, 2010. 2
- Mohamed E Hussein, Marwan Torki, Mohammad A Gowayed, and Motaz El-Saban. Human action recognition using a temporal hierarchy of covariance descriptors on 3d joint locations. In *Twenty-third international joint conference on artificial intelligence*, 2013. 10
- Sadeep Jayasumana, Richard Hartley, Mathieu Salzmann, Hongdong Li, and Mehrtaash Harandi. Kernel methods on riemannian manifolds with gaussian rbf kernels. *IEEE transactions on pattern analysis and machine intelligence*, 37(12):2464–2477, 2015. 11
- Hermann Karcher. Riemannian center of mass and mollifier smoothing. *Communications on pure and applied mathematics*, 30(5):509–541, 1977. 28
- Wilfrid S Kendall. Probability, convexity, and harmonic maps with small image i: uniqueness and fine existence. *Proceedings of the London Mathematical Society*, 3(2):371–406, 1990. 28
- Adnan Mujahid Khan, Korsuk Sirinukunwattana, and Nasir Rajpoot. A global covariance descriptor for nuclear atypia scoring in breast histopathology images. *IEEE journal of biomedical and health informatics*, 19(5):1637–1647, 2015. 10
- Janez Križaj, Vitomir Štruc, and Simon Dobrišek. Combining 3d face representations using region covariance descriptors and statistical models. In *2013 10th IEEE international conference and workshops on automatic face and gesture recognition (FG)*, pages 1–7. IEEE, 2013. 10
- John M Lee. *Riemannian manifolds: an introduction to curvature*, volume 176. Springer Science & Business Media, 2006. 4
- Mingyan Li, Radha Poovendran, and Sreeram Narayanan. Protecting patient privacy against unauthorized release of medical images in a group communication environment. *Computerized Medical Imaging and Graphics*, 29(5):367–383, 2005. 2
- Eyal Lotan, Charlotte Tschider, Daniel K Sodickson, Arthur L Caplan, Mary Bruno, Ben Zhang, and Yvonne W Lui. Medical imaging and privacy in the era of artificial intelligence: myth, fallacy, and the future. *Journal of the American College of Radiology*, 17(9):1159–1162, 2020. 2
- Bingpeng Ma, Yu Su, and Frederic Jurie. Covariance descriptor based on bio-inspired features for person re-identification and face verification. *Image and Vision Computing*, 32(6-7):379–390, 2014. 10
- Tetsu Matsukawa, Takahiro Okabe, Einoshin Suzuki, and Yoichi Sato. Hierarchical gaussian descriptor for person re-identification. In *Proceedings of the IEEE conference on computer vision and pattern recognition*, pages 1363–1372, 2016. 10
- Nina Miolane. *Geometric statistics for computational anatomy*. PhD thesis, Université Côte d’Azur, 2016. 2

- Nina Miolane, Nicolas Guigui, Alice Le Brigant, Johan Mathe, Benjamin Hou, Yann Thanwerdas, Stefan Heyder, Olivier Peltre, Niklas Koep, Hadi Zaatiti, et al. Geomstats: a python package for riemannian geometry in machine learning. *Journal of Machine Learning Research*, 21(223): 1–9, 2020a. 9
- Nina Miolane, Nicolas Guigui, Hadi Zaatiti, Christian Shewmake, Hatem Hajri, Daniel Brooks, Alice Le Brigant, Johan Mathe, Benjamin Hou, Yann Thanwerdas, et al. Introduction to geometric learning in python with geomstats. In *SciPy 2020-19th Python in Science Conference*, pages 48–57, 2020b. 9
- Yanwei Pang, Yuan Yuan, and Xuelong Li. Gabor-based region covariance matrices for face recognition. *IEEE Transactions on circuits and systems for video technology*, 18(7):989–993, 2008. 10
- Xavier Pennec. Intrinsic statistics on riemannian manifolds: Basic tools for geometric measurements. *Journal of Mathematical Imaging and Vision*, 25(1):127–154, 2006. 12
- Xavier Pennec, Pierre Fillard, and Nicholas Ayache. A riemannian framework for tensor computing. *International Journal of computer vision*, 66(1):41–66, 2006. 2, 3
- Xavier Pennec, Stefan Sommer, and Tom Fletcher. *Riemannian geometric statistics in medical image analysis*. Academic Press, 2019. 2, 28
- Matthew Reimherr, Karthik Bharath, and Carlos Soto. Differential privacy over riemannian manifolds. *Advances in Neural Information Processing Systems*, 34, 2021. 2, 3, 8, 9, 10, 11, 26
- Christian P Robert, George Casella, and George Casella. *Monte Carlo statistical methods*, volume 2. Springer, 1999. 26
- Armin Schwartzman. Lognormal distributions and geometric averages of symmetric positive definite matrices. *International Statistical Review*, 84(3):456–486, 2016. 6
- Amr Sharaf, Marwan Torki, Mohamed E Hussein, and Motaz El-Saban. Real-time multi-scale action detection from 3d skeleton data. In *2015 IEEE Winter Conference on Applications of Computer Vision*, pages 998–1005. IEEE, 2015. 10
- Stefan Sommer, François Lauze, Søren Hauberg, and Mads Nielsen. Manifold valued statistics, exact principal geodesic analysis and the effect of linear approximations. In *European conference on computer vision*, pages 43–56. Springer, 2010. 2
- Raghav Subbarao and Peter Meer. Nonlinear mean shift over riemannian manifolds. *International journal of computer vision*, 84(1):1–20, 2009. 2
- Hedi Tabia, Hamid Laga, David Picard, and Philippe-Henri Gosselin. Covariance descriptors for 3d shape matching and retrieval. In *Proceedings of the IEEE conference on computer vision and pattern recognition*, pages 4185–4192, 2014. 2, 10
- Yann Thanwerdas and Xavier Pennec. O (n)-invariant riemannian metrics on spd matrices. *arXiv preprint arXiv:2109.05768*, 2021. 5
- P Thomas Fletcher. Geodesic regression and the theory of least squares on riemannian manifolds. *International journal of computer vision*, 105(2):171–185, 2013. 2

- Oncel Tuzel, Fatih Porikli, and Peter Meer. Region covariance: A fast descriptor for detection and classification. In *European conference on computer vision*, pages 589–600. Springer, 2006. 4, 10, 11
- Oncel Tuzel, Fatih Porikli, and Peter Meer. Human detection via classification on riemannian manifolds. In *2007 IEEE Conference on Computer Vision and Pattern Recognition*, pages 1–8. IEEE, 2007. 10
- Han Xiao, Kashif Rasul, and Roland Vollgraf. Fashion-mnist: a novel image dataset for benchmarking machine learning algorithms. *arXiv preprint arXiv:1708.07747*, 2017. 26
- Jiancheng Yang, Rui Shi, Donglai Wei, Zequan Liu, Lin Zhao, Bilian Ke, Hanspeter Pfister, and Bingbing Ni. Medmnist v2: A large-scale lightweight benchmark for 2d and 3d biomedical image classification. *arXiv preprint arXiv:2110.14795*, 2021. 12
- Florian Yger, Maxime Berar, and Fabien Lotte. Riemannian approaches in brain-computer interfaces: a review. *IEEE Transactions on Neural Systems and Rehabilitation Engineering*, 25(10): 1753–1762, 2016. 2
- Kaicheng Yu and Mathieu Salzmann. Second-order convolutional neural networks. *arXiv preprint arXiv:1703.06817*, 2017. 10
- Paolo Zanini, Marco Congedo, Christian Jutten, Salem Said, and Yannick Berthoumieu. Transfer learning: A riemannian geometry framework with applications to brain–computer interfaces. *IEEE Transactions on Biomedical Engineering*, 65(5):1107–1116, 2017. 2
- Mingyong Zeng, Zemin Wu, Chang Tian, Lei Zhang, and Lei Hu. Efficient person re-identification by hybrid spatiogram and covariance descriptor. In *Proceedings of the IEEE conference on computer vision and pattern recognition workshops*, pages 48–56, 2015. 10
- Ying Zhang and Shutao Li. Gabor-lbp based region covariance descriptor for person re-identification. In *2011 Sixth International Conference on Image and Graphics*, pages 368–371. IEEE, 2011. 10

A Proofs

Consider $k \in \mathbb{N}^*$. In this supplementary material, $\|\cdot\|_{L2}$ and $\langle \cdot, \cdot \rangle_2$ denote the standard Euclidean inner product and the Euclidean norm on vectors. i.e., for all $x, y \in \mathbb{R}^k$

$$\langle x, y \rangle_{L2} = \sum_{i=1}^p x_i y_i.$$

$$\|x\|_{L2} = \sqrt{\langle x, x \rangle_{L2}}.$$

Then, $\langle \cdot, \cdot \rangle_F, \|\cdot\|_F$ denotes Frobenius inner product and Frobenius norm respectively, i.e., given $A, B \in \mathbb{R}^{k \times k}$

$$\langle A, B \rangle_F = \text{Tr}[A^T B].$$

$$\|A\|_F = \sqrt{\langle A, A \rangle_F}.$$

Lastly, $\|\cdot\|_2$ denotes the spectral norm of matrices. i.e., for all $A \in \mathbb{R}^{k \times k}$

$$\|A\|_2 = \sup_{\|x\|_{L2} \neq 0} \frac{\|Ax\|_{L2}}{\|x\|_{L2}}.$$

A.1 Distribution of privacy loss

In this section, we derive the distribution of the privacy loss. Its proof requires us to first introduce the following definitions.

Definition 8 (Diffeomorphism and Isometry). *A diffeomorphism between two manifolds \mathcal{M}_1 and \mathcal{M}_2 is an invertible smooth function whose inverse is also smooth. A diffeomorphism ϕ between two Riemannian manifolds (\mathcal{M}_1, g_1) , (\mathcal{M}_2, g_2) is called an isometry if it preserves distances i.e., $\rho_{g_1}(p, q) = \rho_{g_2}(\phi(p), \phi(q))$ for all $p, q \in \mathcal{M}_1$.*

Note that Logm is a diffeomorphism from $\text{SPD}(k)$ to $\text{SYM}(k)$ and vecd is a diffeomorphism from $\text{SYM}(k)$ to $\mathbb{R}^{\frac{k(k+1)}{2}}$, making vecd Logm a diffeomorphism from $\text{SPD}(k)$ to $\mathbb{R}^{\frac{k(k+1)}{2}}$. Importantly for our derivations in the proofs of this Subsection, the operation vecd Logm preserves the distances – making it an isometry.

Lemma 9 (vecd Logm is an isometry). *Let $\text{Logm} : \text{SPD}(k) \rightarrow \text{SYM}(k)$ be the matrix logarithm and let $\text{vecd} : \text{SYM}(k) \rightarrow \mathbb{R}^{\frac{k(k+1)}{2}}$ be defined as $\text{vecd}(X) = [\text{diag}(X)^T, \sqrt{2} \text{upperdiag}(X)^T]^T$. Then $\text{vecd Logm} : \text{SPD}(k) \rightarrow \mathbb{R}^{\frac{k(k+1)}{2}}$ is an isometry from $\text{SPD}(k)$ equipped with the log-Euclidean metric to standard Euclidean space $\mathbb{R}^{\frac{k(k+1)}{2}}$ with standard L2 metric, i.e.,*

$$\rho_{\text{LE}}(X_1, X_2) = \rho_{L2}(\text{vecd Logm } X_1, \text{vecd Logm } X_2), \quad (7)$$

where $X_1, X_2 \in \text{SPD}(k)$. Hence we have that

$$\|\text{Logm } X\|_F = \|\text{vecd Logm } X\|_{L2}. \quad (8)$$

Proof. Let X_1, X_2 be elements of $\text{SPD}(k)$. We have:

$$\begin{aligned} & \rho_{\text{LE}}^2(X_1, X_2) \\ &= \|\text{Logm } X_1 - \text{Logm } X_2\|_F^2 \\ &= \sum_{i,j}^k (\text{Logm } X_1 - \text{Logm } X_2)_{ij}^2 \\ &= \sum_{i<j}^k (\text{Logm } X_1 - \text{Logm } X_2)_{ij}^2 + \sum_{i>j}^k (\text{Logm } X_1 - \text{Logm } X_2)_{ij}^2 + \sum_{i=j}^k (\text{Logm } X_1 - \text{Logm } X_2)_{ij}^2 \\ &= 2 \cdot \sum_{i<j}^k (\text{Logm } X_1 - \text{Logm } X_2)_{ij}^2 + \sum_{i=j}^k (\text{Logm } X_1 - \text{Logm } X_2)_{ij}^2 \\ &= \left\| \sqrt{2} \text{upperdiag}(\text{Logm } X_1 - \text{Logm } X_2) \right\|_{L2}^2 + \|\text{diag}(\text{Logm } X_1 - \text{Logm } X_2)\|_{L2}^2 \\ &= \|\text{vecd}(\text{Logm } X_1 - \text{Logm } X_2)\|_{L2}^2 \\ &= \|\text{vecd Logm } X_1 - \text{vecd Logm } X_2\|_{L2}^2 \\ &= \rho_{L2}^2(\text{vecd Logm } X_1, \text{vecd Logm } X_2). \end{aligned}$$

from which we have Eq. (7). Eq. (8) follows as

$$\|\text{Logm } X\|_F = \rho_{\text{LE}}(X, I) = \rho_{\text{L2}}(\text{vecd } \text{Logm } X, \text{vecd } \text{Logm } I) = \|\text{vecd } \text{Logm } X\|_{\text{L2}}.$$

□

Now, we prove some useful properties of the Log Gaussian distribution, denoted \mathcal{LN} , that we will use later. Essentially, we show that the Log Gaussian distribution behaves “nicely” with vector space structure of $\text{SPD}(k)$. We recall that the vector space operations on the SPD manifold are defined as follows,

$$X_1 \oplus X_2 = \text{Expm} [\text{Logm } X_1 + \text{Logm } X_2]. \quad (9)$$

$$X_1 \ominus X_2 = \text{Expm} [\text{Logm } X_1 - \text{Logm } X_2]. \quad (10)$$

Lemma 10. *Take $k \in \mathbb{N}$. Let I denote the $k \times k$ identity matrix, and consider $M, C \in \text{SPD}(k)$, $\Sigma \in \text{SPD}(\frac{k(k+1)}{2})$ and χ_d^2 the chi-square distribution with d degrees of freedom. Then:*

$$X \sim \mathcal{LN}(I, \Sigma) \implies X \oplus M \sim \mathcal{LN}(M, \Sigma). \quad (11)$$

$$X \sim \mathcal{LN}(I, \sigma^2 I) \implies \langle \text{Logm } C, \text{Logm } X \rangle_F \sim \mathcal{N}(0, \sigma^2 \|\text{Logm } C\|_F^2). \quad (12)$$

$$X \sim \mathcal{LN}(I, \sigma^2 I) \implies \|\text{Logm } X\|_F^2 \sim \sigma^2 \chi_{\frac{k(k+1)}{2}}^2. \quad (13)$$

Proof. We first recall standard properties of multivariate normal distribution. Let $m, a \in \mathbb{R}^p$ and $\Sigma, I \in \mathbb{R}^{p \times p}$ then following properties hold true.

$$x \sim \mathcal{N}(m, \Sigma) \implies a + x \sim \mathcal{N}(a + m, \Sigma). \quad (14)$$

$$x \sim \mathcal{N}(m, \Sigma) \implies a^T x \sim \mathcal{N}(a^T m, a^T \Sigma a). \quad (15)$$

$$x \sim \mathcal{N}(0, \sigma^2 I) \implies \|x\|_{\text{L2}}^2 \sim \sigma^2 \chi_p^2. \quad (16)$$

where χ^2 denotes chi-square distribution. We prove the properties (a)-(c) below.

(a) Distribution of $X \oplus M$.

$$\begin{aligned} \text{vecd}[\text{Logm}[X \oplus M]] &\stackrel{(*)}{=} \text{vecd}[\text{Logm}[\text{Expm} [\log X + \log M]]] \\ &= \text{vecd}[\text{Logm } X + \text{Logm } M] \\ &= \text{vecd}[\text{Logm } X] + \text{vecd}[\text{Logm } M] \\ &\stackrel{(**)}{\sim} \mathcal{N}(\text{vecd}[\text{Logm } M], \Sigma). \end{aligned}$$

where in (*) we used Eq. 9 and in (**) Eq. (14).

(b) Distribution of $\langle \text{Logm } C, \text{Logm } X \rangle_F$.

$$\begin{aligned} \langle \text{Logm } C, \text{Logm } X \rangle_F &\stackrel{(*)}{=} \langle \text{vecd}[\text{Logm } C], \text{vecd}[\text{Logm } X] \rangle_{\text{L2}} \\ &\stackrel{(**)}{\sim} \mathcal{N}(\langle \text{vecd}[\text{Logm } C], 0 \rangle_{\text{L2}}, \text{vecd}[\text{Logm } C]^T \sigma^2 I \text{vecd}[\text{Logm } C]) \\ &\sim \mathcal{N}(0, \sigma^2 \|\text{vecd}[\text{Logm } C]\|_{\text{L2}}^2) \\ &\stackrel{(*)}{\sim} \mathcal{N}(0, \sigma^2 \|\text{Logm } C\|_F^2). \end{aligned}$$

where we used Eq. 8 in (*) and Eq. 15 in (**).

(c) Distribution of $\|\text{Logm } X\|_F^2$.

$$\|\text{Logm } X\|_F^2 \stackrel{(*)}{=} \|\text{vecd}[\text{Logm } X]\|_{L_2}^2 \stackrel{(**)}{\sim} \sigma^2 \chi_{\frac{k(k+1)}{2}}^2.$$

where we used Eq. 8 in (*) and Eq. 16 in (**) with $p = \frac{k(k+1)}{2}$. \square

As corollary, we give equivalent reformulation of Tangent Gaussian mechanism that will useful in the rest of the proofs.

Corollary 11 (Equivalent Reformulation of Tangent Gaussian). *Let \mathbf{A}_{TG} be a Tangent Gaussian mechanism defined as $\mathbf{A}_{\text{TG}}(f(\mathcal{D})) = X$, $X \sim \mathcal{LN}(f(\mathcal{D}), \sigma^2 I)$. Then, it is equivalently defined as:*

$$\mathbf{A}_{\text{TG}}(f(\mathcal{D})) = f(\mathcal{D}) \oplus N, N \sim \mathcal{LN}(I, \sigma^2 I).$$

Proof. The proof comes from Eq. 11 of Lemma 10. \square

Now, we are ready to prove the distribution of the privacy loss of the Tangent Gaussian Mechanism.

Theorem 12 (Distribution of the privacy loss of the Tangent Gaussian). *Let \mathbf{A}_{TG} be a Tangent Gaussian mechanism with variance σ^2 . Its privacy loss is normally distributed as*

$$L_{\mathbf{A}_{\text{TG}}, \mathcal{D}, \mathcal{D}'} \sim \mathcal{N}\left(\frac{\rho_{\text{LE}}^2(f(\mathcal{D}), f(\mathcal{D}'))}{2\sigma^2}, \frac{\rho_{\text{LE}}^2(f(\mathcal{D}), f(\mathcal{D}'))}{\sigma^2}\right).$$

Proof. Assume that $\mathcal{D}, \mathcal{D}'$ are adjacent datasets. Let $V = f(\mathcal{D}) \ominus f(\mathcal{D}')$. Consider the privacy loss random variable $L_{\mathbf{A}_{\text{TG}}, \mathcal{D}, \mathcal{D}'}$. Let $Y = \mathbf{A}_{\text{TG}}(\mathcal{D})$.

$$\begin{aligned} & \ln\left(\frac{p_{\mathbf{A}_{\text{TG}}(\mathcal{D})}(Y)}{p_{\mathbf{A}_{\text{TG}}(\mathcal{D}')} (Y)}\right) \\ & \stackrel{(1)}{=} \ln\left(\frac{p_{\mathbf{A}_{\text{TG}}(\mathcal{D})}(f(\mathcal{D}) \oplus N)}{p_{\mathbf{A}_{\text{TG}}(\mathcal{D}')} (f(\mathcal{D}) \oplus N)}\right) \\ & \stackrel{(2)}{=} -\frac{1}{2} \left[\text{vecd}\left(\text{Logm}(f(\mathcal{D}) \oplus N) - \text{Logm } f(\mathcal{D})\right) \right]^T \frac{I}{\sigma^2} \text{vecd}\left(\text{Logm}(f(\mathcal{D}) \oplus N) - \text{Logm } f(\mathcal{D})\right) \\ & \quad + \frac{1}{2} \left[\text{vecd}\left(\text{Logm}(f(\mathcal{D}) \oplus N) - \text{Logm } f(\mathcal{D}')\right) \right]^T \frac{I}{\sigma^2} \text{vecd}\left(\text{Logm}(f(\mathcal{D}) \oplus N) - \text{Logm } f(\mathcal{D}')\right) \\ & \stackrel{(3)}{=} -\frac{1}{2\sigma^2} \left\| \text{vecd}\left(\text{Logm } N\right) \right\|_{L_2}^2 + \frac{1}{2\sigma^2} \left\| \text{vecd}\left(\text{Logm } f(\mathcal{D}) - \text{Logm } f(\mathcal{D}') + \text{Logm } N\right) \right\|_{L_2}^2 \\ & \stackrel{(4)}{=} -\frac{1}{2\sigma^2} \left\| \text{vecd}\left(\text{Logm } N\right) \right\|_{L_2}^2 + \frac{1}{2\sigma^2} \left\| \text{vecd}\left(\text{Logm}(V \oplus N)\right) \right\|_{L_2}^2 \\ & \stackrel{(5)}{=} \frac{1}{2\sigma^2} \left[\|\text{Logm}(V \oplus N)\|_F^2 - \|\text{Logm } N\|_F^2 \right] \\ & = \frac{1}{2\sigma^2} \left[\|\text{Logm } V\|_F^2 + 2\langle \text{Logm } V, \text{Logm } N \rangle_F \right] \\ & \stackrel{(6)}{\sim} \frac{1}{2\sigma^2} \left[\|\text{Logm } V\|_F^2 + 2\mathcal{N}\left(0, \sigma^2 \|\text{Logm } V\|_F^2\right) \right] \end{aligned}$$

$$\begin{aligned}
& \stackrel{(7)}{\approx} \mathcal{N} \left(\frac{\|\text{Logm } V\|_F^2}{2\sigma^2}, \frac{\|\text{Logm } V\|_F^2}{\sigma^2} \right) \\
& \stackrel{(8)}{\approx} \mathcal{N} \left(\frac{\rho_{\text{LE}}^2(f(\mathcal{D}), f(\mathcal{D}'))}{2\sigma^2}, \frac{\rho_{\text{LE}}^2(f(\mathcal{D}), f(\mathcal{D}'))}{\sigma^2} \right),
\end{aligned}$$

where we used following properties in each of the steps labeled above.

1. Equivalent reformulation of Tangent Gaussian, Corollary. 11.
2. Density of Log Gaussian Distribution.
3. $f(\mathcal{D}) \oplus N = \text{Expn}[\text{Logm } f(\mathcal{D}) + \text{Logm } N]$.
4. $\text{Logm}(V \oplus N) = \text{Logm } f(\mathcal{D}) - \text{Logm } f(\mathcal{D}') + \text{Logm } N$.
5. Isometry of the vecd operation, Eq.8
6. Eq. 12 in Lemma. 10.
7. standard Gaussian property, see Eq. 14.
8. $\|\text{Logm } V\|_F^2 = \|\text{Logm } f(\mathcal{D}) - \text{Logm } f(\mathcal{D}')\|_F^2 = \rho_{\text{LE}}^2(f(\mathcal{D}), f(\mathcal{D}'))$.

□

The following theorem gives the privacy guarantee of the Tangent Gaussian Mechanism.

Theorem 13 (Privacy Guarantee of the Tangent Gaussian Mechanism). *Consider $f : \mathcal{X}^n \rightarrow \text{SPD}(k)$ with log-Euclidean sensitivity Δ_{LE} .*

1. (Classical) Given $\epsilon, \delta \in (0, 1)$, choosing $\sigma = \Delta_{\text{LE}} \sqrt{2 \ln(1.25/\delta)}/\epsilon$, makes the Tangent Gaussian mechanism (ϵ, δ) -differentially private.
2. (Analytic) Given $\epsilon \geq 0, \delta \in (0, 1)$ and Φ the cumulative distribution of the standard Gaussian, choosing any σ that satisfies $\Phi(\frac{\Delta_{\text{LE}}}{2\sigma} - \frac{\epsilon\sigma}{\Delta_{\text{LE}}}) - \exp(\epsilon) \Phi(\frac{\Delta_{\text{LE}}}{2\sigma} - \frac{\epsilon\sigma}{\Delta_{\text{LE}}}) \leq \delta$ makes the Tangent Gaussian mechanism (ϵ, δ) -differentially private.

Proof. The proof proceeds similarly to the proofs referenced below, by only replacing the standard sensitivity Δ_{L_2} with respect to the Euclidean L_2 metric, by Δ_{LE} :

1. (Classical). See Theorem A.1 (Appendix A Page 261) in Dwork et al. (2014).
2. (Analytic). See Theorem 5 (Section 3) in Balle and Wang (2018).

□

A.2 Sensitivity of the Fréchet Mean and Utility of the Tangent Gaussian mechanism for the Fréchet Mean

In this section, we prove the sensitivity of the Fréchet Mean in Theorem. 14 and then the utility of the Tangent Gaussian Mechanism in Theorem. 15.

Theorem 14 (Sensitivity of the log-Euclidean Fréchet mean). *Given data in $\mathcal{B}_r(M)$ for some $0 < r < \infty$ and $M \in \text{SPD}(k)$, the sensitivity of the log-Euclidean Fréchet mean verifies: $\Delta_{\text{LE}} \leq \frac{2r}{n}$.*

Proof. Consider $k \in \mathbb{N}$, $0 < r < \infty$ and $M \in \text{SPD}(k)$ such that $\mathcal{B}_r(M)$ is a geodesic ball of radius r and center M . Let $\mathcal{D} \sim \mathcal{D}'$ be adjacent datasets of size $n \in \mathbb{N}$ that lie in $\mathcal{B}_r(M)$. Without loss of generality, we can assume that they differ only by their last data point X_n and X'_n : $\mathcal{D} = \{X_1, X_2, \dots, X_n\}$ and $\mathcal{D}' = \{X_1, X_2, \dots, X'_n\}$. Let $\bar{X}_{\mathcal{D}}, \bar{X}_{\mathcal{D}'}$ denote the Fréchet means of \mathcal{D} and \mathcal{D}' for the log-Euclidean metric, which can be expressed in closed forms as mentioned in the main text. The log-Euclidean distance between the Fréchet means writes:

$$\begin{aligned}
& \rho_{\text{LE}}(\bar{X}_{\mathcal{D}}, \bar{X}_{\mathcal{D}'}) \\
& \stackrel{(*)}{=} \left\| \text{Logm} \left(\text{ExpM} \left(\sum_{i=1}^n \frac{\text{Logm } X_i}{n} \right) \right) - \text{Logm} \left(\text{ExpM} \left(\sum_{i=1}^{n-1} \frac{\text{Logm } X_i}{n} + \frac{\text{Logm } X'_n}{n} \right) \right) \right\|_F \\
& = \left\| \frac{1}{n} \sum_{i=1}^{n-1} \text{Logm } X_i - \frac{1}{n} \sum_{i=1}^{n-1} \text{Logm } X_i + \frac{1}{n} \text{Logm } X_n - \frac{1}{n} \text{Logm } X'_n \right\|_F \\
& = \frac{1}{n} \|\text{Logm } X_n - \text{Logm } X'_n\|_F \\
& = \frac{1}{n} \rho_{\text{LE}}(X_n, X'_n).
\end{aligned}$$

$$\Delta_{\text{LE}} = \sup_{\mathcal{D} \sim \mathcal{D}'} \rho_{\text{LE}}(\bar{X}_{\mathcal{D}}, \bar{X}_{\mathcal{D}'}) = \sup_{\mathcal{D} \sim \mathcal{D}'} \frac{1}{n} \rho_{\text{LE}}(X_n, X'_n) \stackrel{(\dagger)}{\leq} \frac{1}{n} [\rho_{\text{LE}}(X_n, M) + \rho_{\text{LE}}(M, X'_n)] \stackrel{(\ddagger)}{\leq} \frac{2r}{n},$$

where we use the closed form for the log-Euclidean Fréchet means in (*), the triangle inequality in (†) and assumption that data lies in $\mathcal{B}_r(M)$ in (‡). \square

Theorem 15 (Utility). *Let \mathbf{A}_{TG} be the (classical) Tangent Gaussian mechanism, $\mathcal{B}_r(M)$ a geodesic ball of radius $0 < r < \infty$ and center $M \in \mathcal{M}$ containing the dataset \mathcal{D} and f the Fréchet mean. The utility of (ϵ, δ) - \mathbf{A}_{TG} is given by:*

$$\begin{aligned}
& \rho_{\text{LE}}^2(f(\mathcal{D}), \mathbf{A}_{\text{TG}}(\mathcal{D})) \sim \sigma^2 \chi_d^2, \\
& \mathbb{E}[\rho_{\text{LE}}^2(f(\mathcal{D}), \mathbf{A}_{\text{TG}}(\mathcal{D}))] = \frac{8r^2 \ln(1.25/\delta)d}{n^2 \epsilon^2} \quad \text{with } d = \dim(\text{SPD}(k)) = \frac{k(k+1)}{2},
\end{aligned}$$

where χ_d^2 represents the chi squared distribution with d degree of freedoms.

Proof. Consider deviation $\rho_{\text{LE}}^2(f(\mathcal{D}), \mathbf{A}_{\text{TG}}(\mathcal{D}))$

$$\begin{aligned} \rho_{\text{LE}}^2(f(\mathcal{D}), \mathbf{A}_{\text{TG}}(\mathcal{D})) &= \|\text{Logm } f(\mathcal{D}) - \text{Logm } \mathbf{A}_{\text{TG}}(\mathcal{D})\|_F^2 \\ &\stackrel{(1)}{=} \|\text{Logm } f(\mathcal{D}) - \text{Logm}(f(\mathcal{D}) \oplus N)\|_F^2 \\ &\stackrel{(2)}{=} \|\text{Logm } N\|_F^2 \\ &\stackrel{(3)}{\approx} \sigma^2 \chi_d^2, \end{aligned}$$

where we use the following properties at each step:

- (1) Corollary. 11.
- (2) $f(\mathcal{D}) \oplus N = \text{ExpM}[\text{Logm } f(\mathcal{D}) + \text{Logm } N]$.
- (3) Eq. 13 of Lemma. 10.

Now we derive expression for $\mathbb{E}[\rho_{\text{LE}}^2(f(\mathcal{D}), \mathbf{A}_{\text{TG}}(\mathcal{D}))]$

$$\begin{aligned} \mathbb{E}[\rho_{\text{LE}}^2(f(\mathcal{D}), \mathbf{A}_{\text{TG}}(\mathcal{D}))] &\stackrel{(1)}{=} \sigma^2 d \\ &\stackrel{(2)}{=} \frac{2\Delta_{\text{LE}}^2 \ln(1.25/\delta)d}{\epsilon^2} \\ &\stackrel{(3)}{\leq} \frac{8r^2 \ln(1.25/\delta)d}{n^2 \epsilon^2}. \end{aligned}$$

where we use following properties at each step:

1. $c \sim \chi_d^2 \implies \mathbb{E}[c] = d$ i.e., expectation of chi squared distributed random variable is number of degrees of freedom.
2. $\sigma = \Delta_{\text{LE}} \sqrt{2 \ln(1.25/\delta)}/\epsilon$ for (ϵ, δ) - \mathbf{A}_{TG} from Theorem. 13.
3. $\Delta_{\text{LE}} \leq \frac{2r}{n}$ from Theorem. 14.

□

A.3 Bounding geodesic radius of covariance descriptor

In this section we derive log-Euclidean geodesic radius of covariance descriptors. We first prove following lemma that relates $\|\text{Logm } X\|_F$ in terms of lower bound on least eigenvalue and upper bound on largest eigenvalue of X .

Lemma 16. *If $X \in \text{SPD}(k)$ and let $\lambda_{\min}(X), \lambda_{\max}(X)$ be the minimum and maximum eigenvalues of X . If $\ell \leq \lambda_{\min}(X)$ and $\lambda_{\max}(X) \leq L$ Then, $\|\text{Logm } X\|_F \leq \sqrt{k} \max\{|\ln \ell|, |\ln L|\}$.*

Proof. Consider,

$$\begin{aligned}
\|\text{Logm } X\|_F &\stackrel{(\dagger)}{\leq} \sqrt{k} \|\text{Logm } X\|_2 \\
&= \sqrt{k} \max_{i=1}^n |\ln \lambda_i| \\
&= \sqrt{k} \max \left\{ \left| \min_{i=1}^n \ln \lambda_i \right|, \left| \max_{i=1}^n \ln \lambda_i \right| \right\} \\
&\stackrel{(\ddagger)}{=} \sqrt{k} \max \left\{ \left| \ln \min_{i=1}^n \lambda_i \right|, \left| \ln \max_{i=1}^n \lambda_i \right| \right\} \\
&= \sqrt{k} \max \{ |\ln \lambda_{\min}|, |\ln \lambda_{\max}| \}. \tag{17}
\end{aligned}$$

where (\dagger) uses the fact that $A \in \mathbb{R}^{k \times k}$, $\|A\|_F \leq \sqrt{k} \|A\|_2$ and (\ddagger) uses the fact that \ln is monotonically increasing. Now, we split the derivation into two cases.

1. CASE $\lambda_{\min}(X) \geq 1$. For $x \geq 1$, $|\ln x|$ is an increasing function, which gives us: $|\ln \ell| \leq |\ln \lambda_{\min}(X)| \leq |\ln \lambda_{\max}| \leq |\ln L|$

$$\sqrt{k} \max \{ |\ln \lambda_{\min}|, |\ln \lambda_{\max}| \} \leq \sqrt{k} |\ln L| = \sqrt{k} \max \{ |\ln \ell|, |\ln L| \}. \tag{18}$$

2. CASE $\lambda_{\min}(X) < 1$. For $x < 1$, $|\ln x|$ is a decreasing function: $|\ln \lambda_{\min}| \leq |\ln \ell|$. We further split the derivation into two sub-cases here

- (a) SUB-CASE $\lambda_{\max} \geq 1$. In this sub-case $|\ln \lambda_{\max}| \leq |\ln L|$ and $|\ln \lambda_{\min}| \leq |\ln \ell|$ from which we have that

$$\sqrt{k} \max \{ |\ln \lambda_{\min}|, |\ln \lambda_{\max}| \} \leq \sqrt{k} \max \{ |\ln \ell|, |\ln L| \}. \tag{19}$$

- (b) SUB-CASE $\lambda_{\max} < 1$. In this sub-case $|\ln L| \leq |\ln \lambda_{\max}| \leq |\ln \lambda_{\min}| \leq |\ln \ell|$.

$$\sqrt{k} \max \{ |\ln \lambda_{\min}|, |\ln \lambda_{\max}| \} \leq \sqrt{k} |\ln \ell| = \sqrt{k} \max \{ |\ln \ell|, |\ln L| \}. \tag{20}$$

Based on Eq. 18, Eq. 19, Eq. 20 and Eq.17. We can conclude the lemma. □

Lemma 17. *Let $R_\eta(\mathcal{I})$ denote the covariance descriptor for image \mathcal{I} for given $\eta > 0$, which is defined as follows ,*

$$R_\eta(\mathcal{I}) = \left[\frac{1}{|\mathcal{S}|} \sum_{\mathbf{x} \in \mathcal{S}} (\phi(\mathcal{I})(\mathbf{x}) - \mu)(\phi(\mathcal{I})(\mathbf{x}) - \mu)^T \right] + \eta \cdot I,$$

with,

$$\phi(\mathcal{I}) = \left[x, y, \mathcal{I}, |\mathcal{I}_x|, |\mathcal{I}_y|, |\mathcal{I}_{xx}|, |\mathcal{I}_{yy}|, \sqrt{|\mathcal{I}_x|^2 + |\mathcal{I}_y|^2}, \arctan \left(\frac{|\mathcal{I}_x|}{|\mathcal{I}_y|} \right) \right].$$

where x, y are grid positions of Image \mathcal{I} , \mathcal{I} denote pixel intensity values, $|\mathcal{I}_x|, |\mathcal{I}_y|$ denotes first order intensity derivatives and $|\mathcal{I}_{xx}|, |\mathcal{I}_{yy}|$ denotes the second order intensity derivatives then following holds,

1. If \mathcal{I} is grayscale image, then $\|\mathbf{R}_\eta(\mathcal{I})\|_2 \leq 12 + \eta$.
2. If \mathcal{I} is RGB image then $\|\mathbf{R}_\eta(\mathcal{I})\|_2 \leq 14 + \eta$.

Proof. We have:

$$\begin{aligned}
\|\mathbf{R}_\eta(\mathcal{I})\|_2 &= \left\| \left[\frac{1}{|\mathcal{S}|} \sum_{\mathbf{x} \in \mathcal{S}} (\phi(\mathcal{I})(\mathbf{x}) - \mu)(\phi(\mathcal{I})(\mathbf{x}) - \mu)^T \right] + \eta \cdot \mathbf{I} \right\|_2 \\
&\stackrel{(1)}{\leq} \frac{1}{|\mathcal{S}|} \sum_{\mathbf{x} \in \mathcal{S}} \|(\phi(\mathcal{I})(\mathbf{x}) - \mu)(\phi(\mathcal{I})(\mathbf{x}) - \mu)^T\|_2 + \|\eta \cdot \mathbf{I}\|_2 \\
&\leq \max_{\mathbf{x} \in \mathcal{S}} \|(\phi(\mathcal{I})(\mathbf{x}) - \mu)(\phi(\mathcal{I})(\mathbf{x}) - \mu)^T\|_2 + \eta \\
&\stackrel{(2)}{=} \max_{\mathbf{x} \in \mathcal{S}} \|(\phi(\mathcal{I})(\mathbf{x}) - \mu)\|_{\text{L}^2}^2 + \eta \\
&\stackrel{(3)}{\leq} \max_{\mathbf{x} \in \mathcal{S}} \|\phi(\mathcal{I})(\mathbf{x})\|_{\text{L}^2}^2 + \eta, \tag{21}
\end{aligned}$$

where we used following properties in each of the steps:

1. Triangle Inequality.
2. For all $a \in \mathbb{R}^p$, the spectral norm of 1-rank matrix aa^T is $\|a\|_{\text{L}^2}^2$.
3. Consider the descriptor $\phi(\mathcal{I}) = \left[x, y, \mathcal{I}, |\mathcal{I}_x|, |\mathcal{I}_y|, |\mathcal{I}_{xx}|, |\mathcal{I}_{yy}|, \sqrt{|\mathcal{I}_x|^2 + |\mathcal{I}_y|^2}, \arctan\left(\frac{|\mathcal{I}_x|}{|\mathcal{I}_y|}\right) \right]$. Then, $\phi(\mathcal{I})(\mathbf{x})_i \geq 0$ for each $\mathbf{x} \in \mathcal{S}$ and $i \in \{1, \dots, k\}$. This yields:
 $(\mu)_i = (|\mathcal{S}|^{-1} \sum_{\mathbf{x} \in \mathcal{S}} \phi(\mathcal{I})(\mathbf{x}))_i \geq 0$. Hence it implies that $\|\phi(\mathcal{I})(\mathbf{x}) - \mu\|_{\text{L}^2}^2 \leq \|\phi(\mathcal{I})(\mathbf{x})\|_{\text{L}^2}^2$.

Then, the following calculations provide an upper bound for $\|\phi(\mathcal{I})(\mathbf{x})\|_2^2$. Specifically, we bound each of the 6 elements constituting the descriptor defined as

$$\phi(\mathcal{I}) = [x, y, \mathcal{I}, |\mathcal{I}_x|, |\mathcal{I}_y|, |\mathcal{I}_{xx}|, |\mathcal{I}_{yy}|, \sqrt{|\mathcal{I}_x|^2 + |\mathcal{I}_y|^2}, \arctan\left(\frac{|\mathcal{I}_x|}{|\mathcal{I}_y|}\right)].$$

1. Normalized grid positions : $\forall \mathbf{x} \in \mathcal{S}, 0 \leq x, y \leq 1$.
2. Pixel intensity values C_i for $i \in [c]$: $\forall \mathbf{x} \in \mathcal{S}, 0 \leq C_i[\mathbf{x}] \leq 1$.
3. First intensity derivatives $|\mathcal{I}_x|, |\mathcal{I}_y|$: The first intensity derivatives can be obtained by the convolution operation (denoted as \star):

$$\mathcal{I}_x = \mathcal{I} \star \frac{1}{4} \begin{pmatrix} +1 & 0 & -1 \\ +2 & 0 & -2 \\ +1 & 0 & -1 \end{pmatrix}, \mathcal{I}_y = \mathcal{I} \star \frac{1}{4} \begin{pmatrix} +1 & +2 & +1 \\ 0 & 0 & 0 \\ -1 & -2 & -1 \end{pmatrix}.$$

Since $0 \leq \mathcal{I}(\mathbf{x}) \leq 1$, using the definition of the convolution operation yields $\forall \mathbf{x} \in \mathcal{S}, |\mathcal{I}_x(\mathbf{x})| \leq 1, |\mathcal{I}_y(\mathbf{x})| \leq 1$.

4. Second intensity derivatives $|\mathcal{I}_{xx}|, |\mathcal{I}_{yy}|$: The second intensity derivatives can be obtained by the convolution operation (denoted as \star)

$$\mathcal{I}_{xx} = \mathcal{I} \star \frac{1}{32} \begin{bmatrix} +1 & 0 & -2 & 0 & 1 \\ +4 & 0 & -8 & 0 & 4 \\ +6 & 0 & -12 & 0 & 6 \\ +4 & 0 & -8 & 0 & 4 \\ +1 & 0 & -2 & 0 & 1 \end{bmatrix}, \mathcal{I}_{yy} = \mathcal{I} \star \frac{1}{32} \begin{bmatrix} +1 & +4 & +6 & +4 & +1 \\ 0 & 0 & 0 & 0 & 0 \\ -2 & -8 & -12 & -8 & -2 \\ 0 & 0 & 0 & 0 & 0 \\ +1 & +4 & +6 & +4 & +1 \end{bmatrix}.$$

Since $0 \leq \mathcal{I}(\mathbf{x}) \leq 1$, using the definition of the convolution operation yields $|\mathcal{I}_{xx}(\mathbf{x})| \leq 1$, $|\mathcal{I}_{yy}(\mathbf{x})| \leq 1$.

5. Norm of first intensity derivatives : since $|\mathcal{I}_x(\mathbf{x})| \leq 1$, $|\mathcal{I}_y(\mathbf{x})| \leq 1$ we have that $\forall \mathbf{x} \in \mathcal{S}$, $\sqrt{\mathcal{I}_x(\mathbf{x})^2 + \mathcal{I}_y(\mathbf{x})^2} \leq \sqrt{2}$.
6. Angle of intensity derivatives : Note that for $a \geq 0$, $0 \leq \arctan a \leq \frac{\pi}{2}$. Hence we have that $\forall \mathbf{x} \in \mathcal{S}$, $\arctan\left(\left|\frac{\mathcal{I}_x(\mathbf{x})}{\mathcal{I}_y(\mathbf{x})}\right|\right) \leq \frac{\pi}{2}$.

These provide the following upper bounds on L2 norm of $\phi(\mathcal{I})(\mathbf{x})$,

$$\text{for a gray scale image, } \forall \mathbf{x} \in \mathcal{S} \|\phi(\mathcal{I})(\mathbf{x})\|_{L_2}^2 \leq 12, \quad (22)$$

$$\text{for RGB image, } \forall \mathbf{x} \in \mathcal{S} \|\phi(\mathcal{I})(\mathbf{x})\|_{L_2}^2 \leq 14. \quad (23)$$

The claim follows by using Eq. 22, Eq. 23 in Eq. 21 □

Theorem 18 (Geodesic Radius of Covariance Descriptors).

1. If \mathcal{I} is a gray scale image, then $\|\text{Logm } \mathbf{R}_\eta(\mathcal{I})\|_F \leq \sqrt{9} \max\{|\ln \eta|, |\ln(12 + \eta)|\}$.
2. If \mathcal{I} is a RGB image, then $\|\text{Logm } \mathbf{R}_\eta(\mathcal{I})\|_F \leq \sqrt{11} \max\{|\ln \eta|, |\ln(14 + \eta)|\}$.

Proof. We first note that

$$\begin{aligned} \lambda_{\min}(\mathbf{R}_\eta(\mathcal{I})) &= \lambda_{\min} \left[\frac{1}{|\mathcal{S}|} \sum_{\mathbf{x} \in \mathcal{S}} (\phi(\mathcal{I})(\mathbf{x}) - \mu)(\phi(\mathcal{I})(\mathbf{x}) - \mu)^T + \eta I \right] \\ &\stackrel{(1)}{\geq} \lambda_{\min} \left[\frac{1}{|\mathcal{S}|} \sum_{\mathbf{x} \in \mathcal{S}} (\phi(\mathcal{I})(\mathbf{x}) - \mu)(\phi(\mathcal{I})(\mathbf{x}) - \mu)^T \right] + \lambda_{\min}[\eta I] \\ &\stackrel{(2)}{\geq} 0 + \eta. \end{aligned} \quad (24)$$

where we used Weyl's inequality for symmetric matrices in (1) and λ_{\min} of positive semi definite matrix is ≥ 0 and $\lambda_{\min}[\eta I] = \eta$ in (2).

For gray scale images, $\mathbf{R}_\eta(\mathcal{I})$ produces a 9×9 matrix:

$$\begin{aligned} \|\text{Logm } \mathbf{R}_\eta(\mathcal{I})\|_F &\stackrel{(*)}{\leq} \sqrt{9} \max\{|\ln \ell|, |\ln L|\} \\ &\stackrel{(**)}{=} \sqrt{9} \max\{|\ln \eta|, |\ln(12 + \eta)|\}, \end{aligned}$$

where we use Lemma. 16 in (*) and Eq.24($\ell = \eta$) and Lemma. 17($L = 12 + \eta$) in (**)
 For RGB images, $R_\eta(\mathcal{I})$ produces a 11×11 matrix:

$$\begin{aligned} \|\text{Logm } R_\eta(\mathcal{I})\|_F &\stackrel{(\dagger)}{\leq} \sqrt{11} \max \{|\ln \ell|, |\ln L|\} \\ &\stackrel{(\ddagger)}{=} \sqrt{11} \max \{|\ln \eta|, |\ln(14 + \eta)|\}, \end{aligned}$$

where we use Lemma. 16 in (\dagger) and Eq.24 ($\ell = \eta$) and Lemma. 17($L = 14 + \eta$) in (\ddagger), in a similar fashion. \square

Note that in all of our experiments, we choose $\eta = 10^{-6}$ and hence $|\ln \eta| \approx 13.8$ dominates over $|\ln(12 + \eta)| \approx 2.5$ and $|\ln(14 + \eta)| \approx 2.6$.

A.4 Implementation Details

Let $k \in \mathbb{N}$, $M \in \text{SPD}(k)$, $\sigma > 0$ and ρ_{LE} denote log-Euclidean distance. The Riemannian Laplace distribution with log-Euclidean distance is given by

$$p(X|M, \sigma) = \frac{1}{\mathcal{C}_{M, \sigma}} \exp\left(-\frac{\rho_{\text{LE}}(X, M)}{\sigma}\right). \quad (25)$$

Note that sampling from Eq. (25) requires Markov Chain Monte Carlo (MCMC) methods Robert et al. (1999), for which one needs to choose a proposal distribution that generates candidates on the SPD Manifold. We choose the Log Gaussian distribution as the proposal in our experiments given its simplicity and the fact that it is quick to sample from. In all experiments, we found that using the log Gaussian distribution as proposal yields a stable acceptance ratio of 50% to 65%. To summarize,

1. Initialize X_{curr} at a random point of the manifold $\text{SPD}(k)$.
2. For $1 \rightarrow n$ iterations
 - (a) Draw a candidate from $X \sim \mathcal{LN}(X_{\text{curr}}, \sigma^2 I)$.
 - (b) With probability $\exp(-\rho_{\text{LE}}(X_{\text{mean}}, X)/\sigma) / \exp(-\rho_{\text{LE}}(X_{\text{curr}}, X)/\sigma)$ accept the generated candidate X and set $X_{\text{curr}} = X$.

The final sample is chosen based on a burn-in period of 50,000 steps.

A.5 Additional Set of Experiments on Real World Datasets

We perform additional experiments that complement the ones presented in the main paper. We choose MNIST, KMNIST Clanuwat et al. (2018) (gray scale images) and CIFAR10, FashionMNIST Xiao et al. (2017) (RGB images) as datasets. We extract images from 4 classes for each dataset and compute the corresponding class-wise Fréchet means of their covariance descriptors ($\eta = 10^{-6}$), which we privatize using the Riemannian Laplace Mechanism Reimherr et al. (2021) and our proposed mechanism Tangent Gaussian (Analytic). Fig. 4 shows the utilities for different values of $\epsilon \in \{0.1, 0.3, 0.5, 0.7, 0.9\}$ and $\delta \in \{10^{-5}, 10^{-7}, 10^{-9}\}$. Each experiment is repeated 10 times, the results are averaged and the (avg-2*std, avg+2*std) band is shown. Fig. 4 illustrates the better utility of our mechanism compared to the Riemannian Laplace mechanism.

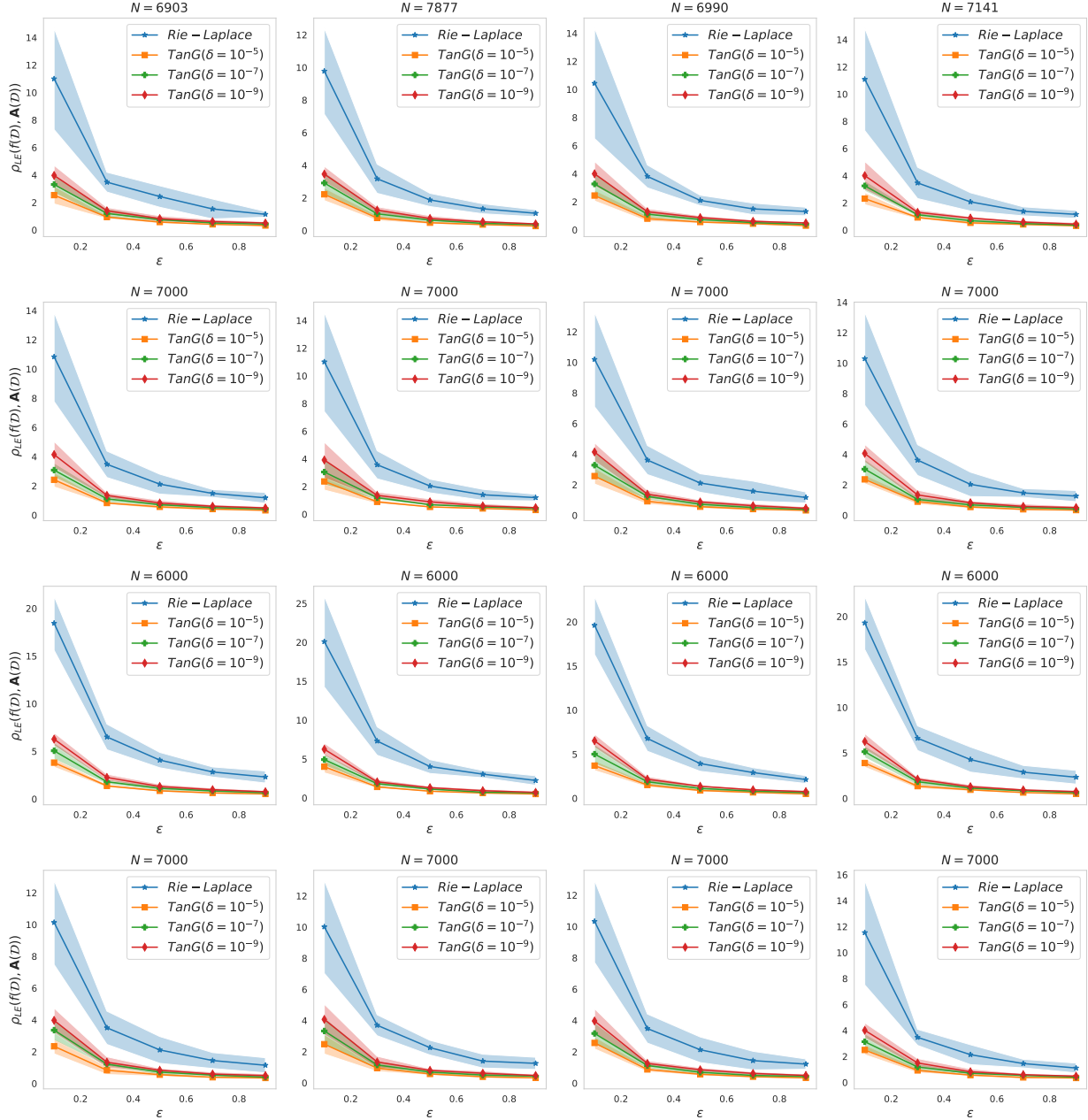


Figure 4: Utilities on the private Fréchet means for different privacy parameters ϵ , and real-world datasets of sizes N . First and Second Row: Fréchet mean from MNIST, KMNIST (Gray scale images yielding 9×9 SPD descriptors). Third and Fourth Row: Fréchet mean from CIFAR10, FashionMNIST (RGB images yielding 11×11 SPD descriptor). *Rie-Laplace* means the Riemannian Laplacian mechanism. *TanG* means the Tangent Gaussian Mechanism for different values of δ (ours). We also show the mean-2*std, mean+2*std bands.

B Fréchet Mean : Pathological Cases

Figure 5 illustrates examples where the Fréchet mean does not exist, or where the Fréchet mean is not unique. Figure 5 (left) shows the punctured plane $\mathbb{R}^2 \setminus \{0,0\}$, defined as a Riemannian

manifold inheriting the Euclidean metric from \mathbb{R}^2 . On this Riemannian manifold, the empirical Fréchet mean of the points $(-1, 0)$ and $(1, 0)$ would be $(0, 0)$ which does not belong to the space; hence the Fréchet mean does not exist. One sufficient condition for the existence of Fréchet mean is completeness Pennec et al. (2019). Even if the Fréchet mean exists, it might not be unique. For instance on the sphere \mathcal{S}^2 , the Fréchet mean of points $(0, 0, -1)$, $(0, 0, 1)$ is entire circle $\{(\cos \theta, \sin \theta, 0) | 0 \leq \theta \leq 2\pi\}$ - see Figure. 5 (right). Conditions related to the uniqueness of the Fréchet mean were first due to Karcher (1977), became improved by Kendall (1990), while Afsari (2011) developed tighter conditions.

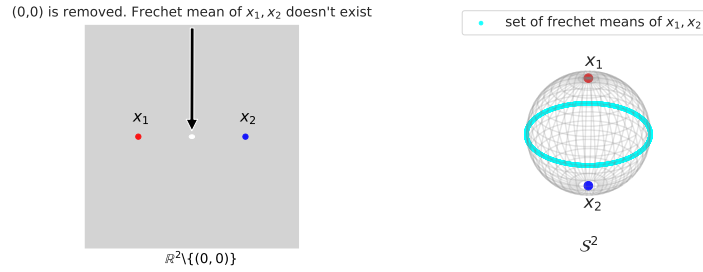


Figure 5: The Fréchet mean does not necessarily enjoy existence and uniqueness as the traditional Euclidean mean. (a) *Non existence of* Fréchet mean in $\mathcal{M} = \mathbb{R}^2 \setminus \{(0, 0)\}$. (b) *Non uniqueness of* Fréchet mean in $\mathcal{M} = \mathcal{S}^2$.